

# AdriaClim

Climate change information, monitoring and management tools for  
adaptation strategies in Adriatic coastal areas

Project ID: 10252001

## D5.4.6 Definition of primary risk information layers to be included in the WP4 geoportal for the Veneto Pilot area

PP02 - ARPA Veneto, PP09 - CMCC

Final version

Public document

June, 2023

Project Acronym: AdriaClim  
Project ID Number: 10252001  
Project Title: Climate change information, monitoring and management tools for adaptation strategies in Adriatic coastal areas  
Priority Axis: 2 - Climate change adaptation  
Specific objective: 2.1 - Improve the climate change monitoring and planning of adaptation measures tackling specific effects, in the cooperation area  
Work Package Number: 5  
Work Package Title: Adaptation Plans  
Activity Number: 5.4  
Activity Title: Veneto Coastal Pilot: Adaptation/Mitigation/Intervention Plan  
Partner in Charge: P02 ARPA Veneto  
Partners involved: P01 CNR, P09 CMCC, P14 AULSS3, P17 COV  
Status: Final  
Distribution: Public  
Date: 30/06/2023

<b>Work Package:</b>	5. Adaptation plans
<b>Activity:</b>	5.4 Veneto Coastal Pilot: Adaptation/Mitigation/Intervention Plan
<b>Deliverable:</b>	D.5.4.6 Definition of primary risk information layers to be included in the WP4 geoportal for the Veneto Pilot area
<b>Authors</b>	ARPA Veneto: Francesco Rech, Giovanni Massaro, Fabio Zecchini; IUAV: Francesco Musco, Denis Maragno, Filippo Magni, Gianfranco Pozzer, Nicola Romanato; CMCC@Ca'Foscari: Silvia Torresan, Maria Katherina Dal Barco, Davide Mauro Ferrario, Ngoc Diep Nguyen, Margherita Maraschini, Heloisa Labella Fonseca, Olinda Rufo, Stefania Gottardo, Andrea Critto.
<b>Due month</b>	M42
<b>Delivery month</b>	M42

## ➤ Table of contents

Table of contents	4
1 Introduction	6
2 ARPA Veneto climate database, processing and sharing atmospheric variables on the Geoportal	8
2.1 The Veneto weather and climate monitoring network	8
2.2 Acquisition, validation and archiving of meteorological-climatic data	15
2.3 Climate normals, indicators and climatological database	17
2.4 Sharing of climate indicators on the geoportal	21
2.5 Tool to visualize climate projections for north-eastern Italy	22
3 Primary risk information layers used to inform climate change impact and adaptation analysis at the regional scale	24
3.1 Atmospheric indicators	25
3.1.1 Temperature related indicators	26
3.1.2 Precipitation related indicators	29
3.1.3 Humidity related indicators	31
3.1.4 Wind related indicators	32
3.1.5 Solar radiation	32
3.1.6 Atmospheric indicators calculated from the regional reanalysis data	33
3.2 Marine indicators	36
3.2.1 Sea level	37
3.2.2 Ocean current velocity	38
3.2.3 Wave regimes	39
3.3 Territorial indicators	42
3.3.1 Land use indicators	42
3.3.2 Coastal protection on shoreline and dune indicators results	46
3.3.3 Subsidence	48
3.3.4 Topographic indicators	50
3.3.5 Soil types	52
3.3.6 Permeability	54
3.3.7 River discharge	57

3.4 Damage indicators	61
4 Primary vulnerability/exposure information layers used to inform climate impacts and adaptation analysis at the local scale	64
4.1 Spatial indicators	64
4.1.1 Vegetation Health Index (VHI)	66
4.1.2 Map of runoff coefficients (MCD)	67
4.1.3 Digital Terrain Model (DTM)	68
4.1.4 Imperviousness Density (IMD)	69
4.1.5 European Settlement Map (ESM)	70
4.1.6 Soil cover and soil cover database (CCS)	72
4.1.7 Urban activities (OSM)	73

## 1 Introduction

The data needed to allow the study of climate and the climatic characterisation of a territory must be homogeneous, measured and archived with the same criteria for an adequately long period of time to allow the availability of a significant sample to allow statistical analysis, and they must also be acquired with a spatial and temporal resolution that is able to characterize the peculiarities of the various environmental systems under study.

In particular, it is important to emphasize the importance of the criteria for measuring weather-climate data (and environmental data in general), which must be standardized over the long term. The same applies to the criteria for the control, maintenance and calibration of measuring instruments. If this is not the case, there is a risk that elements will be artificially introduced that are capable of disrupting measurements and having a significant effect on trends. It should be remembered that, for climatic weather monitoring, the characteristics of the measurement site (type of soil, presence of natural and anthropic obstacles, orographic factors, etc.) are also very important; over periods of more than thirty years, these factors can vary and consequently modify the measurements.

Time series of point data must then be processed in order to provide useful information to support specific decision-making processes. Management information platforms must allow rapid access to summary information such as: general statistical elements (averages, medians, extremes, variances calculated over different time intervals), trends, specific indicators, probability of occurrence of severe events, etc.

The spatial representation of summary data and indicators is also an important tool for representing and studying the territory.

In general, the use of georeferenced information constitutes a basic tool to address the issue of analyzing the impacts of climate change on the territory and in particular to support spatial planning processes.

But consequently is equally relevant the spatial characterisation of exposure and vulnerability correlated to specific hazards, i.e. the factors that allow to assess, with as much detail as possible, the territory's response to the effects caused by the hazards.

The availability of information (as far as possible in standardized formats) to localize and quantify the damage caused by environmental adversities is important to assess cause-effect relations and to focus attention on the hazards that have the greatest impact on a specific territory.

Lastly, the importance of making geo-referenced data on future climate scenarios easily accessible is emphasized, in order to make it possible to assess the possible effects of climate change in terms of potential changes in risk. These information layers should be able to direct the choices of policy-makers, technicians and citizens towards viable and sustainable adaptation solutions not only now but also in the future.

With the Adriaclim project, climate and spatial data management and processing methodologies were developed to meet the above-mentioned needs and an effort was also made to share and align the various partners' databases using shared data organization formats (net.cdf).

In this deliverable, after a short description of the ARPA Veneto climate database and data processing and sharing with the project Geoportal (Section 2), the primary risk information layers used to inform climate change impact and adaptation analysis at the regional scale (Section 3) and at the urban scale (Section 4) are presented.

## 2 ARPA Veneto climate database, processing and sharing atmospheric variables on the Geoportal

The organisation of the database on which to base climatological processing is a fundamental premise for any climatological study. In order to manage climatic data and indicators, ARPA Veneto has worked on the creation of a climatic DataBase, a flexible tool that allows both the continuous updating of indicators and the archiving of climatic normals evaluated over different periods. For the purposes of the AdriaClim Project, ARPA Veneto has also equipped itself with a system for sharing climate outputs on the Project geoportal.

### 2.1 The Veneto weather and climate monitoring network

The ARPAV automatic weather stations have generally been operational since the first months of 1992 (see in more detail the information on the start date of activities reported in Tab.1).

All weather stations operate using solar time all year round (CET or UTC + 1) and mainly measure:

- the **Air Temperature** at 2 meters from the ground by making an (instantaneous) measurement every 15 minutes. The average daily temperature is the average of the 96 measurements taken between 00:15 solar hours of day n and 00:00 of day n + 1. The maximum and minimum temperature of day n are the maximum and minimum values between the 96 daily measurements. The sensor is a linearized thermistor, inserted in a white PVC antiradiant screen, equipped with fins for natural ventilation. The resolution (quantization error) is 0.1 ° C, the measurement uncertainty is  $\pm 0.5$  ° C.



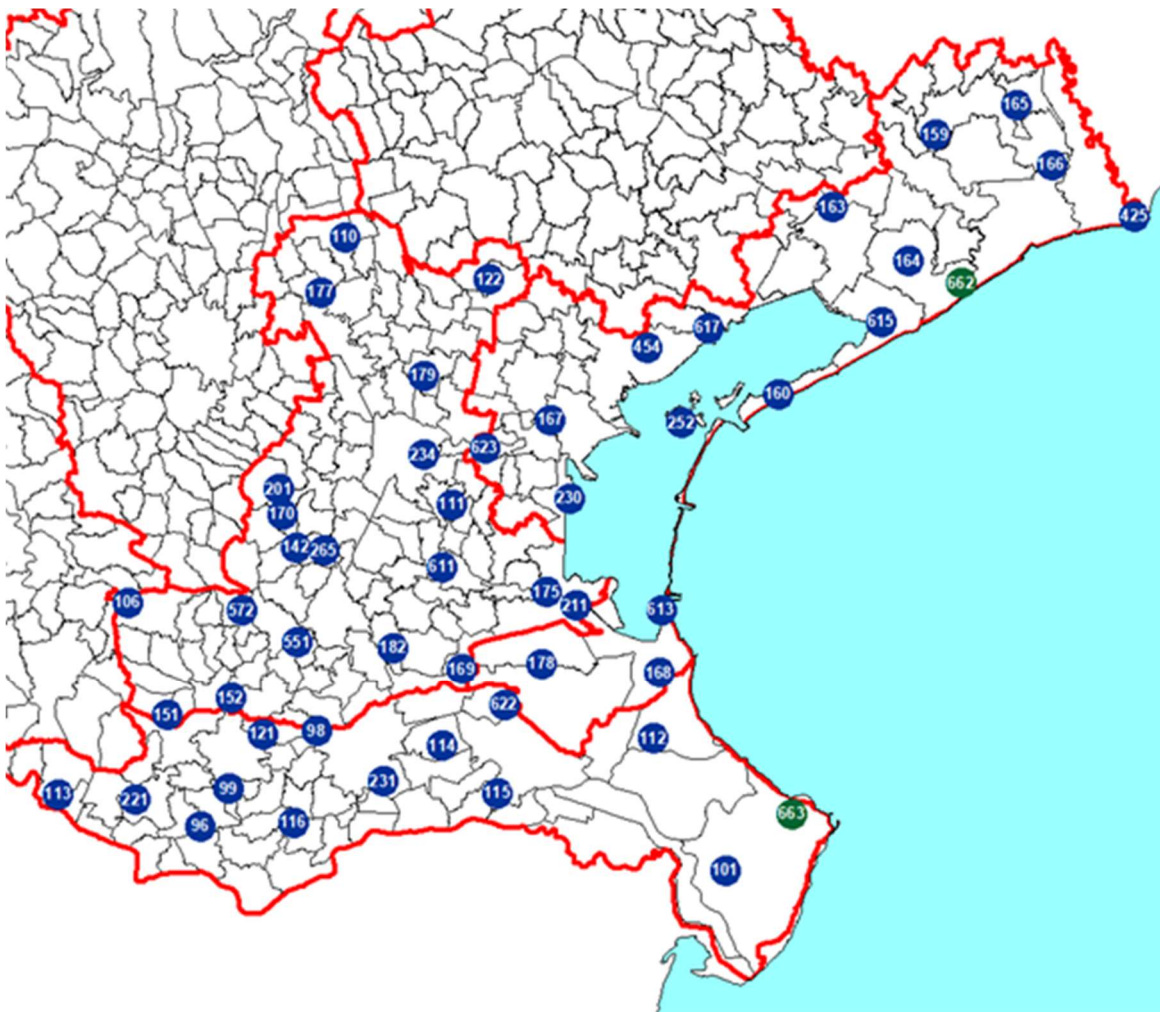


Figure 1 – Veneto Region Provinces of Padua, Rovigo and Venice location of ARPAV automatic weather stations. The blue dots show the code of the stations. The green dots identify the 2 new automatic stations, installed in 2023 near the Adriatic coast with the Adriaclim project (Interreg Italy Croatia Program).

- the **Precipitation** by carrying out a measurement every 5 minutes. The daily precipitation is the sum of the 288 cumulative measurements between the solar hours 00:05 of day n and hours 00:00 of day n + 1. The rain gauge has a calibrated mouth positioned 2 m from the ground, with a surface area of 1000 cm<sup>2</sup>. The measuring system consists of a double oscillating tank which, through a system of funnels, receives the rain from the mouth of the instrument, oscillates when the weight of the collected water reaches 20 g. (therefore it operates as a scale) and subsequently discharges the measured rainfall to the ground. The resolution (quantization error) is 0.2 mm of precipitation. The measurement in 5 minutes is

given by the sum of the oscillations of the trays and is therefore a multiple of 0.2 mm. The measurement error, which can be inferred from the calibration curves, is related to the intensity of the precipitation with an increase in the underestimation of the rain fallen as the intensity increases. On various rain gauge instruments there is a system of electrical resistances that guarantee the heating of the collection funnel when temperatures drop below 0 ° C. This allows the measurement of the equivalent in water of any snowfall.

Additional meteo-climatic variables monitored by the ARPAV automatic stations are:

**Relative Humidity of the air** at 2 m above the ground, making an (instantaneous) measurement every 15 minutes. The data is expressed as a percentage value (%). The capacitive sensor is installed at a height of 2 m from the ground inside a white PVC anti-radiant screen, equipped with fins for natural ventilation, very similar to that of the air temperature sensors.

**Global Solar Radiation** by making a measurement (average of samples taken every 2 seconds) every 15 minutes. The elementary data is expressed in  $Wm^{-2}$ . The sensor is a star pyranometer made up of 72 nickel - chromium thermocouples sheltered by a glass dome. The observed spectral range is included in the range 0,30 , 3,00 *mm*.

For the **Wind variable**, the speed and direction are measured by making a measurement (average of samples taken every 2 seconds) every 10 minutes.

The wind speed data is a 10-minute scaling average of the speed measurements taken every 2 seconds. The data is expressed in  $ms^{-1}$ . The quantization error is  $0.1 ms^{-1}$ . The sensor consists of a three-cup element (Robinson's reel), which rotates around a vertical axis. The rotation speed is proportional to the horizontal wind speed. The three-cup element is connected to a pulse transducer element, integral with the rotation axis, which transforms the rotation speed of the sensor into a digital electrical signal.

The wind direction data is the mode of direction measurements taken every 2 seconds. The data is expressed in sexagesimal degrees (°) referring to the North and indicates the direction of origin of the wind. The quantization error is 3 °.

The sensor consists of a wind vane, which can rotate around a vertical axis, shaped in such a way as to always align itself according to the direction of origin of the wind. The vane is connected to a transducer element, integral with the axis of rotation, which transforms the angular position of the sensor into a digital electrical signal. The transducer element is an optical encoder consisting of a transparent disk with a series of concentric rings with black and white sectors printed on it, arranged so as to represent a Gray type binary sequence (7 bits) along a reading range.

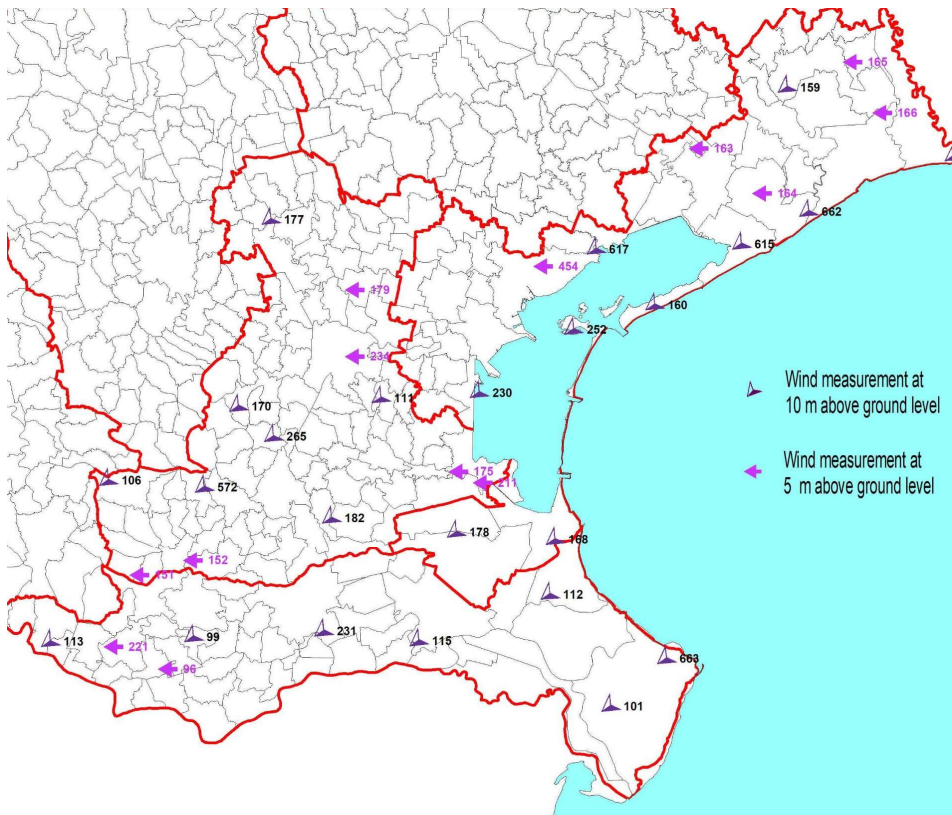


Figure 2 - Veneto Region Province of Padua Rovigo and Venice location of the ARPAV automatic weather stations that measure wind speed and direction at 10 m and 5 m above the ground. To the right of the symbol is the station code with reference to table 1

Ultrasonic wind speed and direction sensors were used in the new installations. The ultrasonic anemometers combined measurement of wind speed and direction. The sensor, whose sensitive part is made up of 3 transducers with a dual function of transmitters and receivers, exploits the principle whereby the acoustic waves, in traveling a certain distance, are influenced by movements of the air passing through.

The sensor simultaneously performs 6 measurements on three different sonic trajectories generating a greater number of measurements and more precise triangulation, especially in the higher ranges, compared to traditional sensors with transducers arranged crosswise to form only 2 acoustic trajectories which allow only 4 simultaneous measurements. This type of sensors have no moving parts.

The wind measurements must be carried out at 10 m from the walking surface in a place without obstacles. Some ARPAV stations, however, carry out wind measurements at 5 m from the ground

(simplified installation) or 2 m from the ground (for agrometeorological measures), obviously these measures are more affected by the friction produced by the ground and the effect of obstacles.

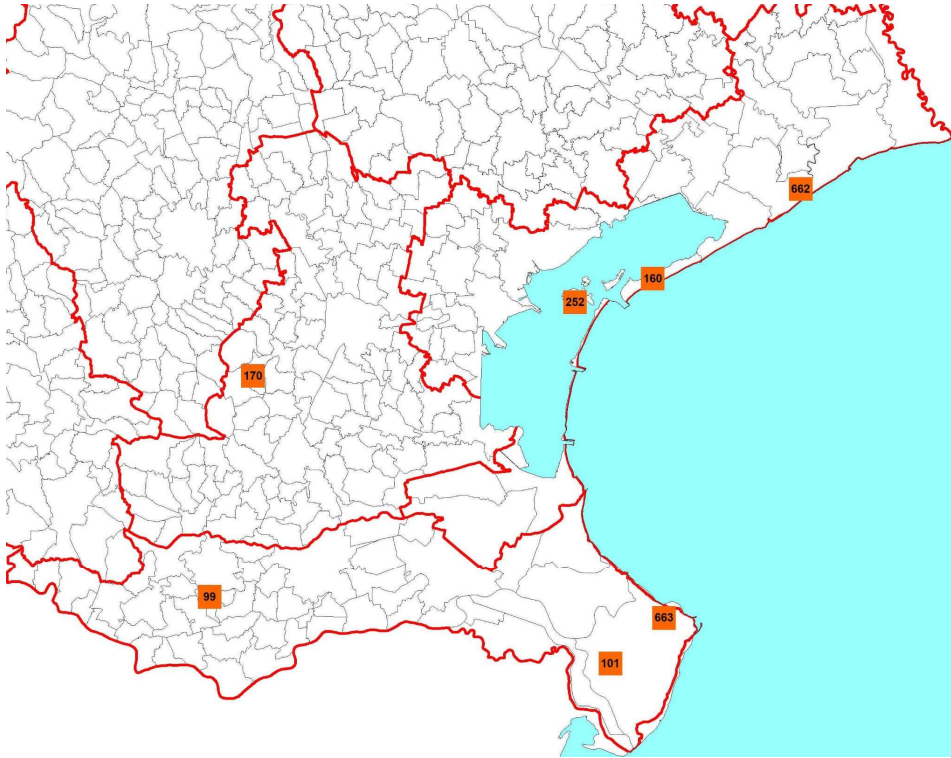


*Figure 3 - Veneto Region, Provinces of Padua, Rovigo and Venice, location of the ARPAV automatic weather stations that measure atmospheric pressure. To the right of the symbol is the station code, with reference to table 1.*

The **Atmospheric Pressure** for monitoring this variable, a measure is acquired every 30 minutes (average of samples taken every 30 seconds). The data is expressed in hPa with a decimal value. The measurements present in SIRAV refer to both the station altitude and reduced to sea level. The measuring instrument is a piezoresistive pressure sensor installed about 1.5 m above the ground.

Other secondary variables are calculated from those measured directly:

- ETO Hargreaves, daily value of potential evapotranspiration processed from temperature data;
- Humidex, processed from data every 15 minutes of temperature and humidity at two metres. Available on an hourly basis.

Table 1a. List of active sensors in the province of Venice. The code and name of the station, the start date of the historical series, the location of the station in geographical coordinates together with the altitude above sea level, the municipality on which it is installed and the reference hydrographic basin are indicated.

Code	Weather station	Operation period	Altitude m (a.s.l.)	Municipality	Province	Geo coordinate EPSG:4258		Basin
		start				Latitude	Longitude	

PROVINCE OF VENEZIA

159	Portogruaro - Lison	01/02/1992	2	PORTOGRUARO	(VE)	45.74549	12.76129	Lemene
160	Cavallino Treporti	01/02/1992	1	CAVALLINO TREPORTI	(VE)	45.45872	12.48626	Drainage basin in the Lagoon of Venice
163	Noventa di Piave - Grossaga	01/02/1992	1	NOVENTA DI PIAVE	(VE)	45.66841	12.58851	Plain between Uivenza and Piave
164	Eraclea	01/02/1992	-1	ERACLEA	(VE)	45.60817	12.70706	Plain between Uivenza and Piave
165	Fossalta di Portogruaro	01/02/1992	3	FOSSALTA DI PORTOGRUARO	(VE)	45.77567	12.89394	Lemene
166	Lugugnana (Portogruaro)	01/02/1992	0	PORTOGRUARO	(VE)	45.70491	12.94669	Lemene
167	Mira	01/02/1992	3	MIRA	(VE)	45.43935	12.11692	Drainage basin in the Lagoon of Venice
168	Chioggia - Sant'Anna	01/02/1992	0	CHIOGGIA	(VE)	45.14632	12.27597	Brenta
178	Cavarzere	01/01/1996	-2	CAVARZERE	(VE)	45.16150	12.08720	Drainage basin in the Lagoon of Venice
230	Campagna Lupia - Valle Averso	17/10/1997	0	CAMPAGNA LUPIA	(VE)	45.34942	12.14156	Drainage basin in the Lagoon of Venice
252	Venezia - Istituto Cavaris	01/03/2000	18	VENEZIA	(VE)	45.42997	12.32810	Drainage basin in the Lagoon of Venice
425	Bibione	13/02/2008	0	SAN MICHELE AL TAGLIAMENTO	(VE)	45.64137	13.07747	Tagliamento
454	Favaro Veneto	21/05/2009	2	VENEZIA	(VE)	45.51731	12.27848	Drainage basin in the Lagoon of Venice
613	Chioggia (centro)	18/12/2020	2	CHIOGGIA	(VE)	45.21813	12.28305	Brenta
615	Jesolo - Cortellazzo	12/02/2021	2	IESOLO	(VE)	45.53585	12.65882	Drainage basin in the Lagoon of Venice
617	Marcon loc. Zuccarello	24/07/2021	1	MARCON	(VE)	45.53739	12.37831	Drainage basin in the Lagoon of Venice
623	Strà	18/12/2020	9	STRA	(VE)	45.41067	12.00851	Drainage basin in the Lagoon of Venice
662	Eraclea - Torre di Fine	17/03/2023	-1	ERACLEA	(VE)	45.57572	12.79133	Plain between Uivenza and Piave

Table 1b. List of active sensors in the province of Padova. The code and name of the station, the start date of the historical series, the location of the station in geographical coordinates together with the altitude above sea level, the municipality on which it is installed and the reference hydrographic basin are indicated.

Code	Weather station	Operation period	Altitude m (a.s.l.)	Municipality	Province	Geo coordinate EPSG:4258		Basin
		Start				Latitude	Longitude	
<b>PROVINCE OF PADOVA</b>								
106	Montagnana	01/11/1990	12	MONTAGNANA	(PD)	45.24777	11.42279	Brenta
110	Cittadella	01/09/1991	50	CITTADELLA	(PD)	45.65647	11.79355	Brenta
111	Legnaro	01/07/1991	7	LEGNARO	(PD)	45.34735	11.95217	Drainage basin in the Lagoon of Venice
122	Trebaseleghe	11/07/1995	23	TRBASELEGHE	(PD)	45.60240	12.02574	Drainage basin in the Lagoon of Venice
142	Faedo (Cinto Euganeo)	01/09/1994	250	CINTO EUGANEO	(PD)	45.30472	11.69772	Brenta
151	Masi	01/05/1994	9	MASI	(PD)	45.11740	11.48088	Brenta
152	Baldovina (Sant'Urbano)	01/05/1994	7	SANT'URBANO	(PD)	45.13473	11.58416	Brenta
169	Agna	02/02/1992	1	AGNA	(PD)	45.15926	11.95776	Drainage basin in the Lagoon of Venice
170	Teolo	02/02/1992	155	TEOLO	(PD)	45.34273	11.67713	Brenta
175	Codevigo	01/02/1992	0	CODEVIGO	(PD)	45.24367	12.09971	Drainage basin in the Lagoon of Venice
177	Grantorto	01/12/1991	32	GRANTORTO	(PD)	45.59472	11.75218	Brenta
179	Campodarsegò	03/02/1992	16	CAMPODARSEGÒ	(PD)	45.49552	11.91336	Drainage basin in the Lagoon of Venice
182	Tribano	01/01/1996	3	TRIBANO	(PD)	45.18669	11.84880	Drainage basin in the Lagoon of Venice
201	Monte Grande (Teolo)	16/01/1995	465	TEOLO	(PD)	45.36192	11.67282	Brenta
211	Codevigo - Ca' di Mezzo	20/06/1996	1	CODEVIGO	(PD)	45.22690	12.14506	Drainage basin in the Lagoon of Venice
234	Padova	01/05/2000	12	PADOVA	(PD)	45.40496	11.90848	Brenta
265	Galzignano - Ca' Demia	15/10/2004	3	GALZIGNANO	(PD)	45.30014	11.74269	Drainage basin in the Lagoon of Venice
551	Sant'Elena	10/07/2013	8	SANT'ELENA	(PD)	45.19660	11.69454	Brenta
572	Ospedaletto Euganeo	27/01/2016	9	OSPEDALETTO EUGANEO	(PD)	45.23456	11.60649	Brenta
611	Bovolenta	17/12/2020	8	BOVOLENTA	(PD)	45.27657	11.93263	Drainage basin in the Lagoon of Venice

Table 1c. List of active sensors in the province of Rovigo. The code and name of the station, the start date of the historical series, the location of the station in geographical coordinates together with the altitude above sea level, the municipality on which it is installed and the reference hydrographic basin are indicated.

Code	Weather station	Operation period	Altitude m (a.s.l.)	Municipality	Province	Geo coordinate EPSG:4258		Basin
		Start				Latitude	Longitude	

#### PROVINCE OF ROVIGO

96	Bagnolo di Po - Pelizzare	01/01/1989	6	BAGNOLO DI PO	(RO)	44.98945	11.52951	Fiszero Tartaro Canal Bianco
98	Conca di rame (Rovigo)	01/01/1989	6	ROVIGO	(RO)	45.09314	11.72082	Fiszero Tartaro Canal Bianco
99	San Bellino	01/01/1989	6	SAN BELLINO	(RO)	45.03150	11.57663	Fiszero Tartaro Canal Bianco
101	Porto Tolle - Pradon	04/01/1989	-3	PORTO TOLLE	(RO)	44.91734	12.36910	Po
112	Rosolina - Po di tramontana	18/02/1992	-2	ROSOLINA	(RO)	45.07114	12.26178	Fiszero Tartaro Canal Bianco
113	Castelnuovo Bariano	01/03/1992	10	CASTELNUOVO BARIANO	(RO)	45.03102	11.30253	Fiszero Tartaro Canal Bianco
114	Villadose	01/03/1992	0	VILLADOSE	(RO)	45.07145	11.92221	Fiszero Tartaro Canal Bianco
115	Adria - Bellombra	01/02/1992	-1	ADRIA	(RO)	45.01568	12.00768	Fiszero Tartaro Canal Bianco
116	Frassinelle Polesine	01/02/1992	4	FRASSINELLE POLESINE	(RO)	44.99058	11.67864	Fiszero Tartaro Canal Bianco
121	Lusia	07/07/1995	6	LUSIA	(RO)	45.09242	11.63364	Fiszero Tartaro Canal Bianco
221	Trecenta	26/05/1993	9	TRECENTA	(RO)	45.02167	11.42663	Fiszero Tartaro Canal Bianco
231	Sant'Apollinare (Rovigo)	01/01/1998	2	ROVIGO	(RO)	45.03840	11.82597	Fiszero Tartaro Canal Bianco
622	Pettorazza Grimani loc. Botti Barbarighe	17/12/2020	2	PETTORAZZA	(RO)	45.11638	12.02445	Drainage basin in the Lagoon of Venice
663	Pila - Porto Peschereccio (Porto Tolle)	15/04/2023	1	PORTO TOLLE	(RO)	44.97805	12.47959	Po

○

## 2.2 Acquisition, validation and archiving of meteorological-climatic data

The data detected by the stations are transmitted via radio to the acquisition center. Currently, a selection of stations is queried every hour to get a real-time picture of the meteorological situation in Veneto, while the remaining stations transmit their complete daily archive after midnight.

The data, both at the acquisition scan and as hourly and daily derived values, are stored in an ARPAV database called SIRAV (Veneto Regional Environmental Information System), which is a relational database in an ORACLE environment.

A specific application called VALIDAZIO allows a group of technicians to carry out the daily control of consistency and quality of the data activating, if necessary, the interventions of the maintenance teams.

Dipartimento Regionale per la Sicurezza del Territorio  
Servizio Centro Meteorologico di Teolo

arpav

**Dati ad intervalli vari sulla rete agro-idro-meteorologica**

Intervallo dati  Giornaliero  Orario  Frequenza di acquisizione  
 Fascia oraria su dati orari  
 Fascia oraria su dati a frequenza

Data di inizio  (gg/mm/aaaa)  
 Data di fine  (gg/mm/aaaa)

Formato output  HTML  CSV  
 Indirizzo e-mail  (obbligatorio con formato CSV)

Attenzione che con il formato CSV i file sono MOLTO grossi e la mail relativa NON parte se si superano i 4 MB di file!  
 Per fare un conto è sufficiente sommare i caratteri di [nome stazione]+[nome sensore]+[data]+[ora]+[valore]+6 e moltiplicare per il numero degli intervalli corrispondenti al periodo scelto.

Elenco di sensori Selezione indicata  
 Mostra dati ricostruiti  Si  No

Per i sensori fare doppio click sulla stazione.

Codice	Stazione
115	Adria - Bellombra [funziona dal 01/02/1992]
169	Agna [funziona dal 02/02/1992]
78	Agno a Recoaro [funziona dal 01/09/1986 al 31/05/2008]
19	Agordo [funziona dal 16/02/1984]

- Direzione vento a 10m (SETTORE) media vettoriale [funziona dal 01/04/2014]
- Direzione vento a 10m (gradi) media vettoriale [funziona dal 01/04/2014]
- Direzione vento a 5m (SETTORE) media vettoriale [funziona dal 16/02/1984 al 01/04/2014]
- Direzione vento a 5m (gradi) media vettoriale [funziona dal 16/02/1984 al 01/04/2014]
- Direzione vento prevalente a 10m (SETTORE) valore [funziona dal 01/04/2014]
- Direzione vento prevalente a 10m (gradi) valore [funziona dal 01/04/2014]

Figure 4. Example of SIRAV DB interface containing all sampling rate data of all sensors, as well as their grouping and processing, supplemented by the master data of station points and individual sensors.

This application, thanks to automatic procedures and easy graphical representations, helps operators to identify absence of data, format errors, exceeding the instrumental range values, exceeding values such as 10 and 90 percentile, excessive persistence of data with the same value, and excessive variations of the data in a limited period of time. In addition, the VALIDAZIO program allows the technicians to make comparisons between trends of different sensors of the same station (eg presence of leaf wetness if rain is recorded or relationships between changes in temperature and relative humidity of the air) and between trends of the same sensor on nearby stations. Comparisons are also possible between the images of the meteorological radar and the point values measured by the rain gauges. It is specified that the VALIDAZIO program carries out automatic reports but the final decision to validate or modify or cancel a data lies with the technician.



## 2.3 Climate normals, indicators and climatological database

Of the more than 200 active measuring stations in the Veneto region, about 110 have a 30-year history series and are suitable for climatological processing. In the coastal provinces of Venice, Padua and Rovigo, there are a total of 24 stations with at least 30 years of operation.

The calculation of climate normals and indicators is done by means of procedures and functions written in Python language, which query the SIRAV database to extract the data and reprocess it to produce and save locally the tables to be used for populating the climate database.

As far as climatic normals are concerned, these are calculated as follows:

- the metadata of the sensors are imported from SIRAV, with all the information needed to select them on the basis of the period of operation and the measured variable;
- the 30-year period 1991-2020 is then identified as the period of interest over which to calculate the climatology;
- then begins, for each sensor, the import of daily data clipped in the period of interest, with a check on the actual number of data available;
- the data are analysed and grouped over several time intervals to form climate normals. For the calculation of daily-scale normals, a 5-day moving window is used to define the mean value and the 10th, 25th, 75th and 90th percentiles.
- The output file is saved and used to populate the climate database tables.

The Python scripts that perform the operations for calculating climate indicators are composed of several nested or sequential functions, starting with the connection to the SIRAV database for the collection of sensor records and the definition of the period over which the indicators are to be calculated: whether over the entire year, a season or a month.

The code continues by calling up various functions for the calculation of temperature and precipitation indicators. Initially, for each sensor, daily data are imported from the SIRAV database and the values are selected according to the required period.

After calculating the percentage of available data, we first calculate the indicators that are based on thresholds only and, after querying the climate database, we calculate the indicators that arise from the comparison between the data and the values of the climatic normal. In fact, the calculation of some indicators, based on percentiles for example, requires having the populated climate database already available. It follows that, temporally, the calculation of indicators is a step later than the identification of climate normals and their storage in the database.

The files are available to create graphs, maps or tables and to be imported into the dedicated table within the climate database on the MySQL server and queried.

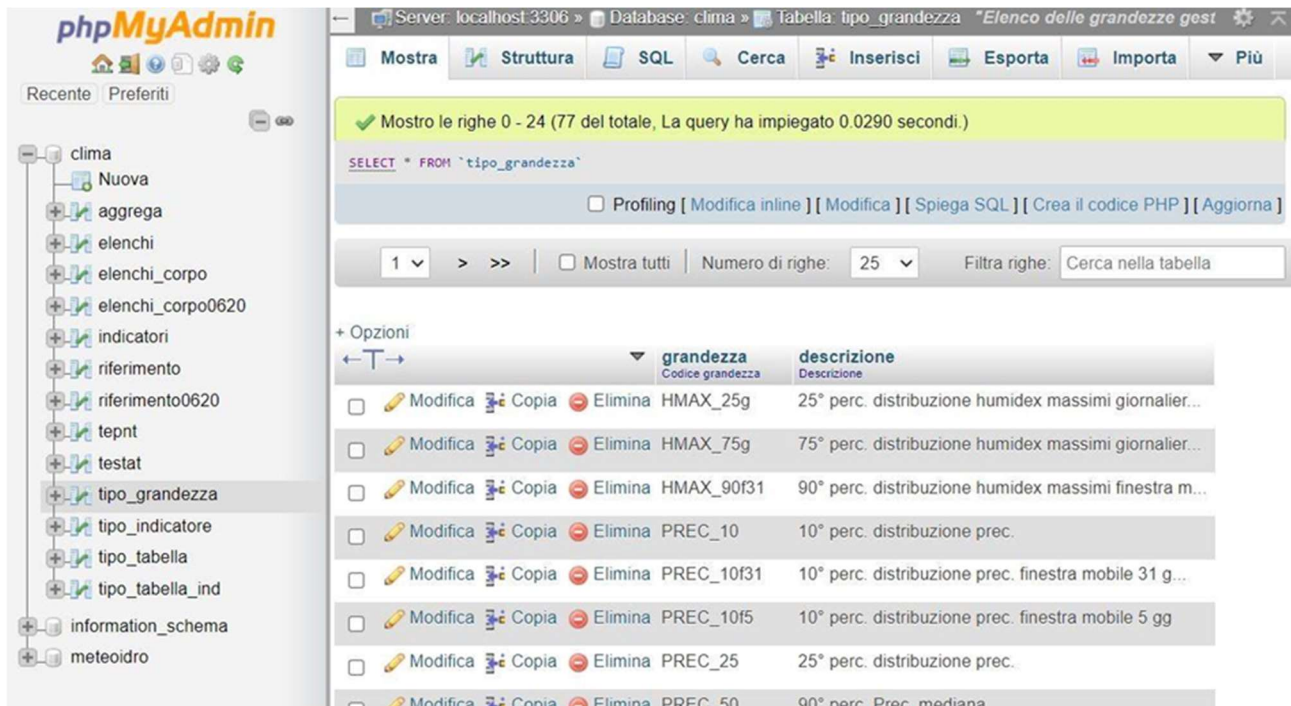


Figure 5. Example of the phpMyAdmin interface of the MySQL database used to organise the tables of weather normals and indicators.

In order to obtain easily comprehensible information on the trend of parameters or weather-climate indicators over an area, it is useful to spatialise point values. For spatialisation, the kriging function in R is used, which is used within a larger Python language code that has the task of customising the parameters to be spatialised, the period to be analysed and the conditions on the choice of measurement points (such as data availability), choosing the spatialisation domain and processing the output produced in R.

The spatialisation procedure consists of several steps:

- input. The first table that is imported into the code is the table of point measurements of the variable or indicator to be spatialised. The table is constructed by querying the climate database. The point data file consists of columns containing the station code, its coordinates and altitude, which will be used as an auxiliary variable in the spatialisation, and the variable to be spatialised:

- grid. A regular grid is adopted on which the point data is spatialised. This is imported as a table consisting of latitude, longitude and elevation columns, derived from a digital terrain model. The grid can be customised by choosing its resolution (0.5 to 5 km), domain (North-East or Veneto) and applying, if necessary, a mask to select only the area of interest;
- spatialisation. Averaged values for the period are spatialised annually. Maps of averages over several years are obtained by averaging the annual maps. spatialisation is performed in R with the Universal Kriging function and using altitude as an auxiliary variable. In the creation of the theoretical variogram (spherical model), which attempts to fit the points of the experimental variogram, the parameters psill, range and nugget are calculated to minimise the residuals at the measurement points:
  - nugget, corresponds to the variance value at zero distance;
  - sill, corresponds to the constant value of the variogram when the variables do not influence each other;
  - range, is the distance at which the value of one point becomes spatially independent of another;
  - psill, is the difference between sill and nugget.

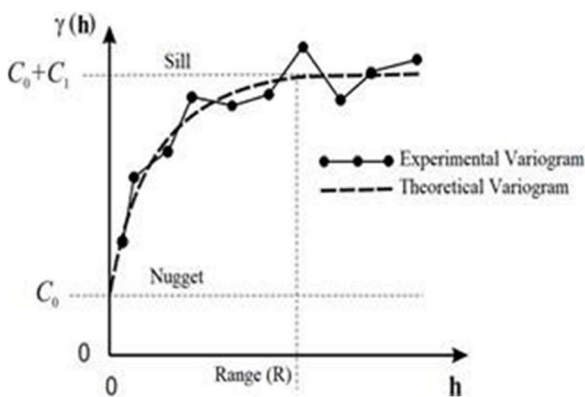


Figure 6. Graphical parameter display for the definition of the theoretical variogram

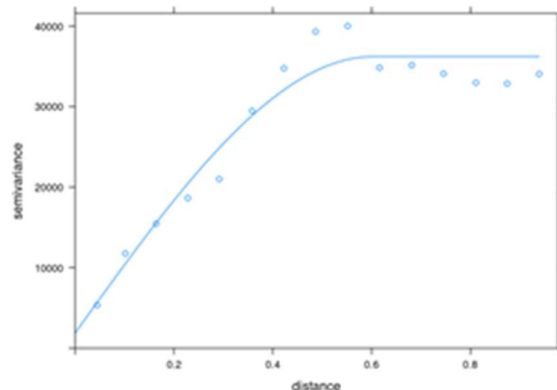


Figure 7. Theoretical variogram adapted to the experimental variogram

The last part of the R script, once the theoretical variogram that best describes the experimental variogram has been found, is to apply the kriging function to spatialise the point data on the chosen grid.

- post-processing. For some indicators, particularly related to the temperature variable, a *coastline effect* was added, which has an influence up to 5 km from a fictitious line that runs along the coast and halves the Venice lagoon. A gradient is sought between stations within 10 km of the coast. The resulting map is merged with the spatialised map by linearly decreasing the influence from the coastline up to 5 km inland.
- Storage. The annual maps are finally collected within netCDF-type files containing metadata.

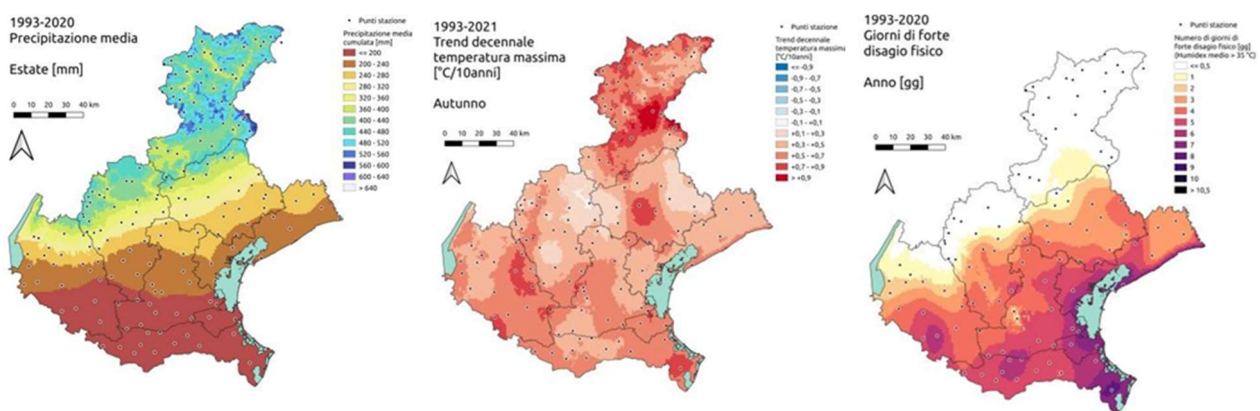


Figure 8. Examples of spatialisation obtained with the described method. The three images were printed with Qgis, which allows the import and processing of netCDF type files. In order, the regional trend of the average summer precipitation over the period 1993-2020 is depicted; the ten-year trend of the autumn maximum temperature over the period 1993-2021; and the number of days of severe physical discomfort per year over the period 1993-2020.

○

## 2.4 Sharing of climate indicators on the geoportal

Arpav has published the developed climatic indicators in its public web-server Thredds: <https://thredds.arpa.veneto.it/thredds/catalog/TDd/nc/catalog.html>

As reported in D.4.2.1, they are: PRCPTOT (total precipitation), R95pTOT (Number of days with cumulative precipitation exceeding that of the 95° perc.), RX1day (Maximum 1-day precipitation amount), RX5day (Maximum 5-days precipitation amount), SDII (simple daily intensity index), SU30 (Summer days), TDd (Mean daily temperature), TNd (Average minimum temperature), TR (Tropical nights), TX90p (Hot days), Txd (Average maximum temperature), WSDI (Warm Spell Duration Index).

They are given in terms of annual or seasonal time series, anomalies and trends as a gridded dataset over Venice province.

set	data	graph	files	AdriaClim Indicators   ARPAE   Porto Garibaldi - Yearly 95% percentile values for sea surface salinity: 2009-2022	🔍	F	I	M	background	📄	🔗	ARPAE	ARPAE_1d9b_9d93_b55e
set	data	graph	files	AdriaClim Indicators   ARPAE   Porto Garibaldi - Yearly maximum values for sea level: 2009-2022	🔍	F	I	M	background	📄	🔗	ARPAE	ARPAE_0333_a949_8d3d
set	data	graph	files	AdriaClim Indicators   ARPAE   Porto Garibaldi - Yearly mean values for sea level: 2009-2022	🔍	F	I	M	background	📄	🔗	ARPAE	ARPAE_c09b_16e3_7611
set	data	graph	files	AdriaClim Indicators   ARPAE   Porto Garibaldi - Yearly minimum, mean, maximum values for sea surface salinity: 2009-2022	🔍	F	I	M	background	📄	🔗	ARPAE	ARPAE_ea36_7e5f_118d
set	data	graph	files	AdriaClim Indicators   ARPAFVG   Temperature, Salinity, Sea Surface Height Pilot Area FVG	🔍	F	I	M	background	📄	🔗	ARPAFVG	ARPAFVG_1a11_be39_413b
set	data	graph	files	AdriaClim Indicators   ARPAV   CDD anomaly seasonal 1992-2011	🔍	F	I	M	background	📄	🔗	ARPA Veneto	indicators_e843_54ff_f8a3
set	data	graph	files	AdriaClim Indicators   ARPAV   CDD anomaly yearly 1992-2011	🔍	F	I	M	background	📄	🔗	ARPA Veneto	indicators_47e0_61e2_a783
set	data	graph	files	AdriaClim Indicators   ARPAV   CDD seasonal 1991-2022	🔍	F	I	M	background	📄	🔗	ARPA Veneto	indicators_a889_9525_2314
set	data	graph	files	AdriaClim Indicators   ARPAV   CDD trend seasonal 1992-2011	🔍	F	I	M	background	📄	🔗	ARPA Veneto	indicators_d43c_27c7_e3de
set	data	graph	files	AdriaClim Indicators   ARPAV   CDD trend yearly 1992-2011	🔍	F	I	M	background	📄	🔗	ARPA Veneto	indicators_9ab1_d3d1_5093
set	data	graph	files	AdriaClim Indicators   ARPAV   CDD yearly 1991-2022	🔍	F	I	M	background	📄	🔗	ARPA Veneto	indicators_e9d2_3394_721a
set	data	graph	files	AdriaClim Indicators   ARPAV   HWN anomaly seasonal 1992-2011	🔍	F	I	M	background	📄	🔗	ARPA Veneto	indicators_9aca_475b_e733
set	data	graph	files	AdriaClim Indicators   ARPAV   HWN anomaly yearly 1992-2011	🔍	F	I	M	background	📄	🔗	ARPA Veneto	indicators_92f5_8181_693e
set	data	graph	files	AdriaClim Indicators   ARPAV   HWN seasonal 1991-2022	🔍	F	I	M	background	📄	🔗	ARPA Veneto	indicators_b95d_586d_36e0
set	data	graph	files	AdriaClim Indicators   ARPAV   HWN trend seasonal 1992-2011	🔍	F	I	M	background	📄	🔗	ARPA Veneto	indicators_c1ce_058d_33e7
set	data	graph	files	AdriaClim Indicators   ARPAV   HWN trend yearly 1992-2011	🔍	F	I	M	background	📄	🔗	ARPA Veneto	indicators_2cd5_abcb_33c0
set	data	graph	files	AdriaClim Indicators   ARPAV   HWN yearly 1991-2022	🔍	F	I	M	background	📄	🔗	ARPA Veneto	indicators_b453_00ab_844f
set	data	graph	files	AdriaClim Indicators   ARPAV   HWTXdx anomaly yearly 1992-2011	🔍	F	I	M	background	📄	🔗	ARPA Veneto	indicators_d52f_e734_1efa
set	data	graph	files	AdriaClim Indicators   ARPAV   HWTXdx trend yearly 1992-2011	🔍	F	I	M	background	📄	🔗	ARPA Veneto	indicators_0a1d_5d8a_8334
set	data	graph	files	AdriaClim Indicators   ARPAV   HWTXdx yearly 1991-2022	🔍	F	I	M	background	📄	🔗	ARPA Veneto	indicators_3beb_7125_15e5
set	data	graph	files	AdriaClim Indicators   ARPAV   R95pDAY anomaly monthly 1992-2011	🔍	F	I	M	background	📄	🔗	ARPA Veneto	indicators_3dfe_0189_5c46
set	data	graph	files	AdriaClim Indicators   ARPAV   R95pDAY anomaly seasonal 1992-2011	🔍	F	I	M	background	📄	🔗	ARPA Veneto	indicators_3fe2_f9d4_46c8
set	data	graph	files	AdriaClim Indicators   ARPAV   R95pDAY anomaly yearly 1992-2011	🔍	F	I	M	background	📄	🔗	ARPA Veneto	indicators_3687_f0cf_7520
set	data	graph	files	AdriaClim Indicators   ARPAV   R95pDAY monthly 1991-2022	🔍	F	I	M	background	📄	🔗	ARPA Veneto	indicators_cc5e_0950_0ecf
set	data	graph	files	AdriaClim Indicators   ARPAV   R95pDAY seasonal 1991-2022	🔍	F	I	M	background	📄	🔗	ARPA Veneto	indicators_02a1_8341_c3d5
set	data	graph	files	AdriaClim Indicators   ARPAV   R95pDAY trend monthly 1992-2011	🔍	F	I	M	background	📄	🔗	ARPA Veneto	indicators_7bb6_d136_b4ff
set	data	graph	files	AdriaClim Indicators   ARPAV   R95pDAY trend seasonal 1992-2011	🔍	F	I	M	background	📄	🔗	ARPA Veneto	indicators_2945_2cce_5ab3
set	data	graph	files	AdriaClim Indicators   ARPAV   R95pDAY trend yearly 1992-2011	🔍	F	I	M	background	📄	🔗	ARPA Veneto	indicators_eb1a_af00_0056
set	data	graph	files	AdriaClim Indicators   ARPAV   R95pDAY yearly 1991-2022	🔍	F	I	M	background	📄	🔗	ARPA Veneto	indicators_52a9_dffa_dc4d
data		graph	files	AdriaClim Indicators   B04, Brunt-Vaisala Frequency   historical	🔍	F	I	M	background	📄	🔗	UNIBO	B04_ecee_2fb4_438c
data		graph	files	AdriaClim Indicators   B04, Brunt-Vaisala Frequency   projection	🔍	F	I	M	background	📄	🔗	UNIBO	B04_07f1_f985_5f84
data		graph	files	AdriaClim Indicators   B04, Brunt-Vaisala Frequency   reanalysis	🔍	F	I	M	background	📄	🔗	UNIBO	B04_8b91_5277_2a92
data		graph	files	AdriaClim Indicators   B04, Brunt-Vaisala Frequency   reanalysis trend	🔍	F	I	M	background	📄	🔗	UNIBO	B04_8395_62bd_31a9
data		graph	files	AdriaClim Indicators   B04, Brunt-Vaisala Frequency   trend historical	🔍	F	I	M	background	📄	🔗	UNIBO	B04_e938_927b_51c9
data		graph	files	AdriaClim Indicators   B04, Brunt-Vaisala Frequency   trend projection	🔍	F	I	M	background	📄	🔗	UNIBO	B04_24b8_654d_97a8
data		graph	files	AdriaClim Indicators   B04, Max Brunt-Vaisala Frequency   historical	🔍	F	I	M	background	📄	🔗	UNIBO	B04_c9e6_9ee5_32c8
data		graph	files	AdriaClim Indicators   B04, Max Brunt-Vaisala Frequency   projection	🔍	F	I	M	background	📄	🔗	UNIBO	B04_8b21_a153_7b5b

Figure 9. Climate indicators developed and shared by Arpav in the project Erddap <https://erddap-adriaclim.cmcc-opa.eu/erddap/info/>.

These datasets have been made available also in the project Erddap <https://erddap-adriaclim.cmcc-opa.eu/erddap/info/> via a federation between the catalogs from Arpav Thredds and CMCC Erddap, by sharing only the metadata and leaving at the Arpav node the data.

The project Geoportal reads in turn the datasets published on Erddap.

## 2.5 Tool to visualize climate projections for north-eastern Italy

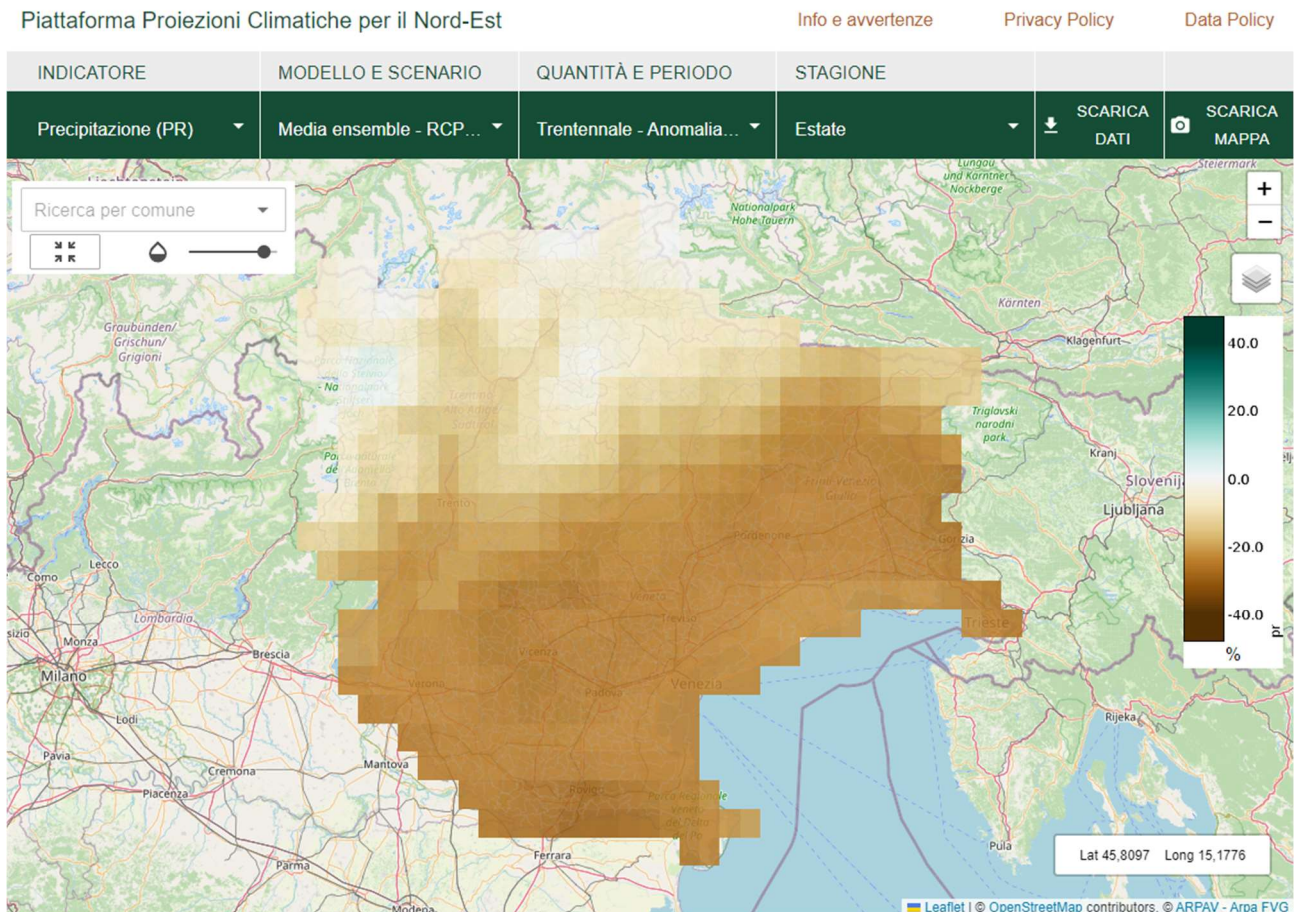


Figure 10. Example of graphic restitution of the Platform: percentage anomaly of summer precipitation in the 30-year period 2071-2100 compared to the historical period 1976-2005.

Arpav, by exploiting both the WP4 knowledge on the data sharing system Erddap and fundings from other projects, has developed <https://clima.arpa.veneto.it>, a totally open-source web-gis platform on regional climate projections specifically suited for North-East Italy. The platform gives access to climate indicators in terms of maps, time series for specific locations, as well as gridded data (Netcdf) and point data (csv). It could be also further developed with the integration of historical climate data from regional weather networks and possibly other datasets (eg.: vulnerability, exposure, risk). This platform gives information on climate hazards at regional scale and it is aimed to support stakeholders, decision makers, citizens with respect to territorial planning, adaptation measures fostering the knowledge and awareness of climate change at local scale.

The underlying informatics infrastructure is based on inter-operable services, among of INSPIRE Directive Network Services and Open Geospatial Consortium services (e.g. WMS, WCS, Opendap) and can be federated with distributed network of DAP nodes (e.g.: Erddap, Thredds, Hyrax).

### 3 Primary risk information layers used to inform climate change impact and adaptation analysis at the regional scale

This Deliverable, carried out within Activity 5.4, is aimed at describing climate risk information layers to inform climate change impacts, as part of the WP4 geoportal for the Veneto Pilot area. Specifically, this section reports the progress of the activities related to the characterization and pre-processing of indicators, focusing on the calculation of hazard, triggering factor, exposure, vulnerability, and impact variables, henceforth defined as indicators. As a consequence, they will be integrated in the multi-risk assessment model developed to define climate-driven damages in the coastal areas of the Veneto Pilot (Deliverable D5.4.5).

In this Section, we present a detailed description of the retrieved indicators (e.g., definition, method of calculation, source), as well as the results of their calculation for the reference period (2009-2020). In particular, the indicators are presented based on macro-categories (Figure 11), concerning atmospheric (Section 3.1), marine (3.2), territorial (Section 3.3), and damage classes (Section 3.4).

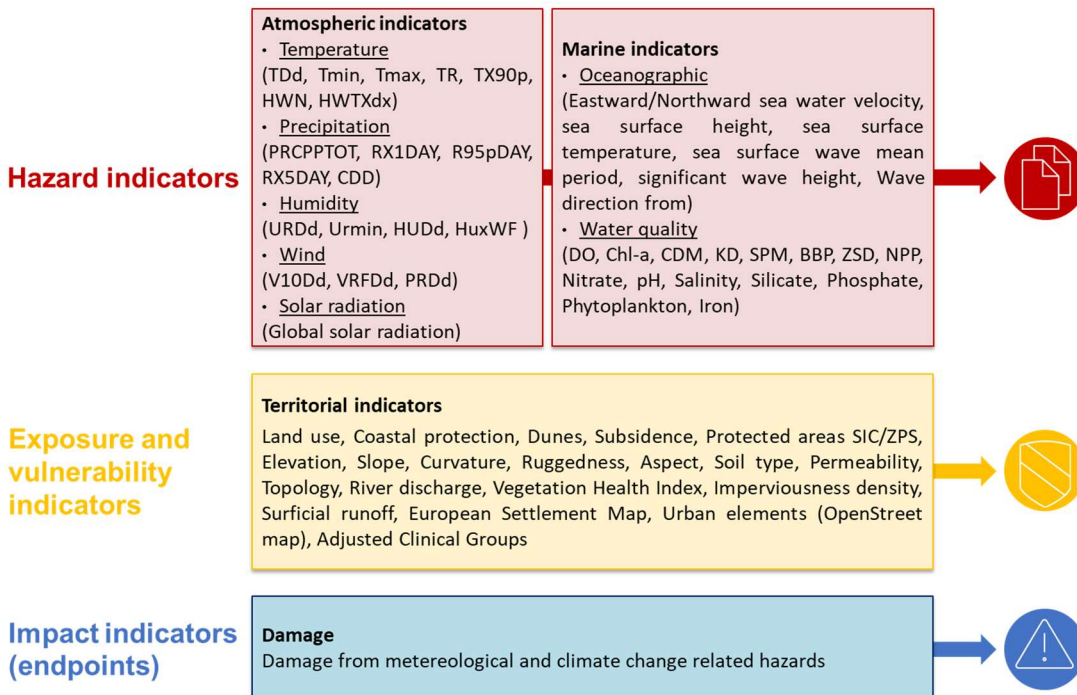


Figure 11. List of indicators available for the Pilot case of the Veneto coastal municipalities.



### 3.1 Atmospheric indicators

This section describes the atmospheric characteristics in the coastal municipalities of the Veneto pilot related to temperature, precipitation, humidity, wind, and solar radiation. All the indicators calculated for the reference period derive from ARPAV meteorological stations that are located homogeneously on the Veneto Region territory. Data are available in the period 2000-2019. The total number of ARPAV stations is 180 of which 20 are located in the coastal zone (up to 20 km landward respect the shoreline). The typology of the data acquired is station-dependent but typically all stations are set to acquire precipitation, temperature, humidity, wind and solar radiation data at hourly or daily base.

Within the boundaries of the 11 coastal municipalities considered in the analysis, there are 9 meteorological stations (i.e., Bibione, Lugugnana, Eraclea, Cavallino-Treporti, Favaro Veneto, Venezia - Istituto Cavanis, Chioggia - Sant'Anna, Rosolina - Po di Tramontana, and Porto Tolle – Padron), as depicted in Figure 12. Among the coastal municipalities, 3 do not have a meteorological station within their territory, namely Jesolo, Porto Viro, and Ariano nel Polesine.

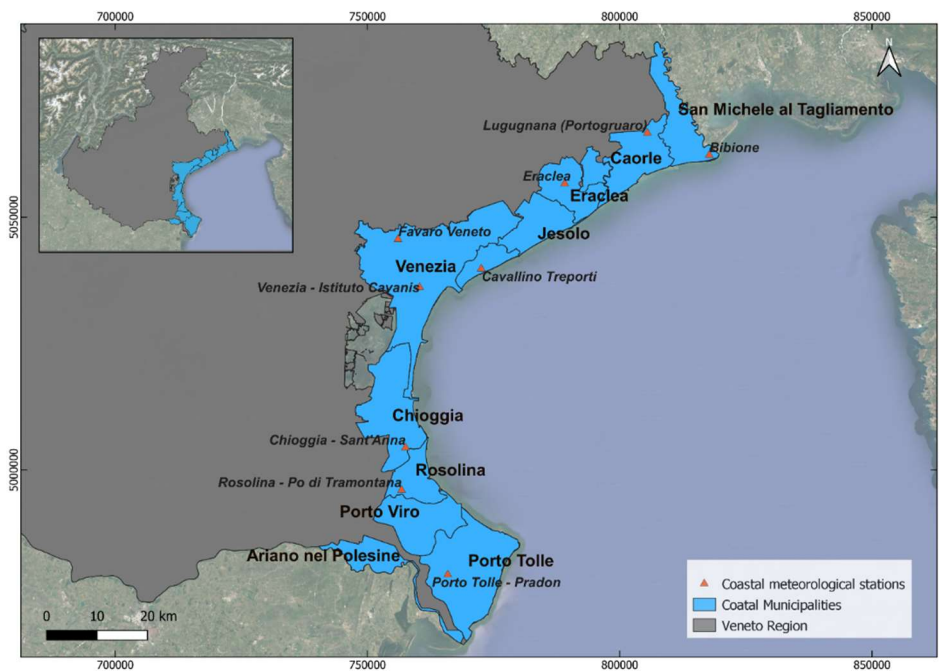


Figure 12. Coastal municipalities of Veneto Region and their meteorological stations.

Considering the proximity of the municipalities and the low variation in the values of the atmospheric parameters, in accordance with the data provider, we applied the nearest neighbours' rule to infer their atmospheric conditions. In particular, we calculated two closest stations' average values or replaced them with values of the closest station. On the other hand, Venezia has 2 stations

within its territory, and similar values were recorded, except for humidity. Therefore, they are interchangeable in the analysis. However, since specific parameters in 2009 and 2017 at the Favaro Veneto station are missing, we decided to use only the Venezia - Istituto Cavanis for the consistency of the analysis, knowing that it is atypical station (located in the city centre, without any adjacent tree, and with the elevation of the sensors at over 20 m).

The data are available under the form of punctual (station-based) and interpolated (raster) data (covering the entire Veneto region). The temporal resolutions of the atmospheric indicators used as inputs for the risk assessment is based on daily, monthly, or yearly values at the municipality level. We extracted the highest temporal resolution available for each indicator and calculated the mean, maximum and minimum values using pandas library in Python (McKinney, 2010). At the first stage of the risk analysis from extreme events in coastal municipalities, we only considered the scalar data, instead of interpolated raster ones, for temperature, precipitation, humidity, wind and solar radiation.

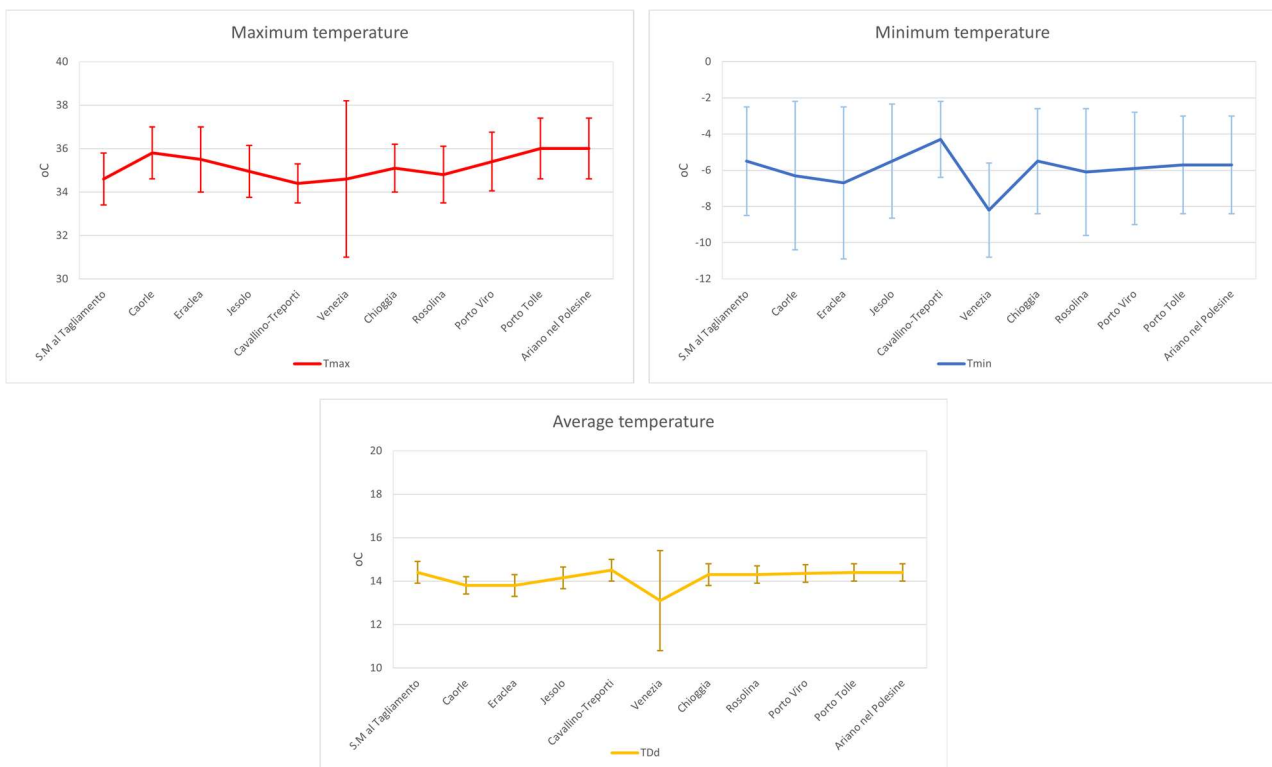
The sections below represent all the indicators generally at their annual average values for the reference period, from 2009 to 2019 based on the granularity and availability of damage data for the reference scenario. The annual mean, maximum and minimum were selectively calculated for each indicator of each year. Then, the average and standard deviation of each municipality were derived for the whole reference period (2009-2019) and represented below.

### 3.1.1 Temperature related indicators

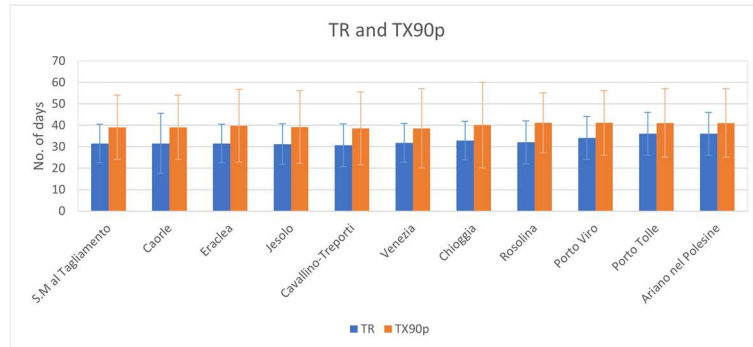
Temperature is one of the most important factors influencing the climate and is often used as headline index in climate models (Crespi et al., 2020). Temperature related indicators strongly relate to heatwaves and droughts and are also influencing factors to water quality changes and eutrophication by the intensification of the hydrological cycle and the alteration of biogeochemical processes linked to warming air temperature (Coffey et al., 2019; Paul et al., 2019; USGCRP, 2017). Considering that these indicators are vital in human health, agricultural and aquaculture, and ecosystems studies.

The temperature related indicators that can be useful for the implementation of climate change risk assessment for the Veneto pilot, include temperature and extreme temperature. The temperature indicators express the trends of the mean, minimum, and maximum temperature, whose annual and seasonal changes have certain influences on the ecosystems and various human activities (Crespi et al., 2020). The extreme temperature indicators, on the other hand, have an important role to identify extreme heat event, and is a triggering factor to drought, which is essential to ecosystems and to many sectors and activities, such as human health, agriculture, aquaculture, construction, transport, and energy (Crespi et al., 2020).

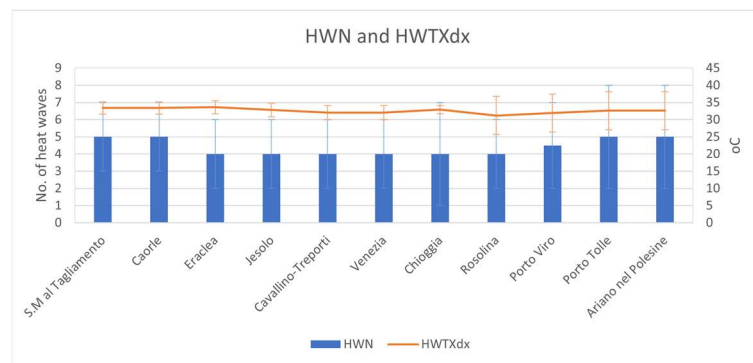
The annual average temperature-related indicators of the 11 coastal municipalities for the period 2009-2019 are shown in Figure 13. In general, the coastal municipalities have an annual average temperature (TDd) of around 14.1°C. While there is a relatively low variation in the average temperature for the period 2009-2019 (average of 0.6°C), the maximum (Tmax) and minimum (Tmin) temperatures have higher variation (average of 1.5 and 3.1°C, respectively). The maximum temperatures range from  $34.4 \pm 0.9^\circ\text{C}$  (Cavallino-Treporti) to  $36 \pm 1.4^\circ\text{C}$  (Porto Tolle and Ariano nel Polesine), whereas the minimum temperatures range from  $-8.2 \pm 2.6^\circ\text{C}$  (Venezia) to  $-4.3 \pm 2.1^\circ\text{C}$  (Cavallino-Treporti) (Figure 13a). The municipalities' average annual tropical nights (TR) and hot days (TX90p) are approximately 33 and 40 days, with the interannual variation of 10 and 16 days, respectively. There is not much variation in the number of hot days between the municipalities (39-41 days), whereas the number of tropical nights ranges from the lowest of  $31 \pm 10$  (Cavallino-Treporti and Jesolo) to the highest of  $36 \pm 10$  (Porto Tolle and Ariano nel Polesine) (Figure 13b). There is an average of 4-5 ( $\pm 2-3$ ) heatwaves (HWN) a year with an average heatwave temperature (HWTXdx) of  $32.6^\circ\text{C}$  ( $\pm 1.2-5.5$ ) for the whole study area (Figure 13c).



(a)



(b)



(c)

Figure 13. The temperature related indicators of 11 coastal municipalities averaged for the reference period 2009-2019. (a) Annual temperature, including the maximum ( $T_{max}$ ), average ( $TDd$ ), and minimum ( $T_{min}$ ) temperatures. (b) TR and TX90p: blue and orange columns represent tropical nights (TR) and hot days (TX90p), respectively. (c) HWN and HWTXdx: the blue columns are the number of heat waves (HWN), while the orange line is the heat wave temperature in Celsius degrees (HWTXdx). Vertical line bars represent the standard deviation over the reference period of the indicators.

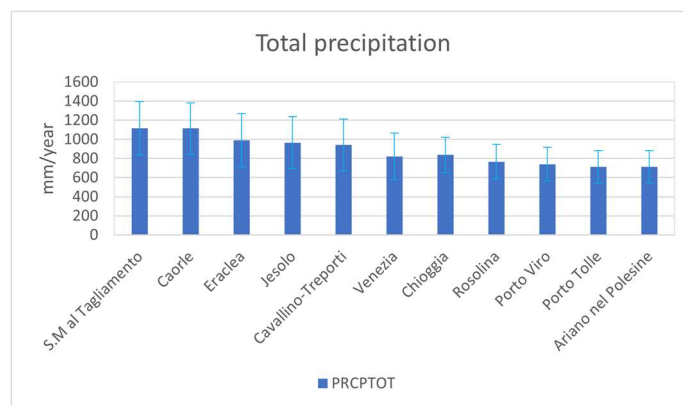
### 3.1.2 Precipitation related indicators

Aside from temperature, precipitation is often used as a headline indicator for climate models for its essential role in determining the climate characteristics of a region (Crespi et al., 2020). Considering precipitation related indicators in multi-risk assessment, they are drivers to drought, pluvial flood, and hydrologic processes. Changes in precipitation and runoff influence physical-chemical status of surface water by the direct transfer of pollutants and thermal energy, and eventually, leading to changes in water quality, and eutrophication (Coffey et al., 2019; Paul et al., 2019; USGCRP, 2017). Changes in precipitation related indicators have specific effects on

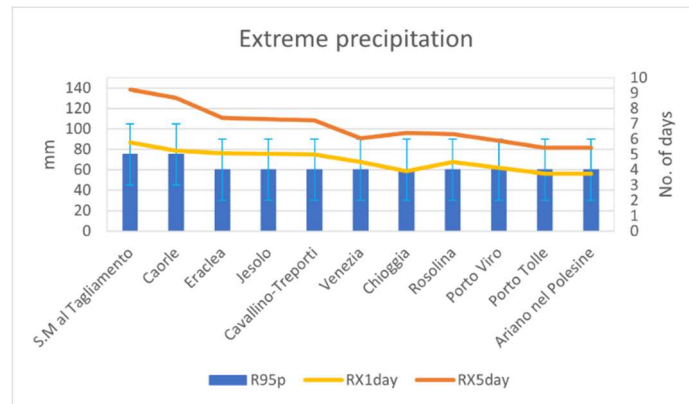
agriculture, aquaculture, ecosystems, and damages to properties and infrastructures of various sectors.

The precipitation related indicators that can be useful for the implementation of climate change risk assessment for the Veneto pilot, include precipitation and extreme precipitation. Annual and seasonal changes in the precipitation indicators are useful for climate change assessments and for various sectoral applications (Crespi et al., 2020). Whereas extreme precipitation indicators are important to evaluate extreme wet and dry conditions, such as pluvial floods and droughts (Crespi et al., 2020).

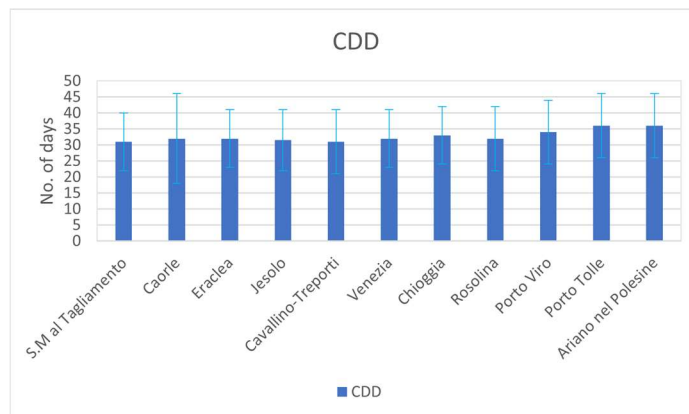
Precipitation related indicators of the 11 coastal municipalities are shown in Figure 14 as annual average values for the period 2009-2019. There is a clear trend that the northern municipalities are wetter and experience higher precipitation than the southern ones. The annual precipitation (PRCPTOT) ranges from  $713.7 \pm 170.1$  mm/year (Porto Tolle and Ariano nel Polesine) to  $1115.8 \pm 277.5$  mm/year (San Michele al Tagliamento) which increase from south to north (Figure 14a). The study area has an average of 4-5 ( $\pm 2$ ) days with extreme precipitation (R95p), whereas their magnitude increases northward. In particular, the average values of RX1day and RX5day range from  $56.2 \pm 15.5$  mm and  $81.7 \pm 19$  mm, respectively, in Ariano nel Polesine and Porto Tolle, to  $86.8 \pm 17.6$  mm and  $138.3 \pm 42$ , respectively, in San Michele al Tagliamento (Figure 14b). The average cumulative dry days (CDD) for the study area is about 33 days/year, with a variation of 10 days for 2009-2019. Similarly, the northern municipalities have fewer cumulative dry days (31-32 days) while that of the southern municipalities are higher (33-36 days; Figure 14c).



(a)



(b)



(c)

Figure 14. Precipitation related indicators of 11 coastal municipalities averaged for the reference period 2009-2019: (a) Total precipitation; (b) RX1day, RX5day and R95p; and (c) CDD. Vertical line bars represent the standard deviation over the reference period of the indicators.

### 3.1.3 Humidity related indicators

Humidity is the concentration of water vapour present in the air, which depends on the temperature and pressure of the system (American Meteorological Society, 2021). The assessment of the combination of temperature and humidity are essential to human health and agriculture due to hazards such as heatwaves and droughts.

Humidity related indicators averaged for the period 2009-2019 of the 11 coastal municipalities are shown in Figure 15. The average humidex (HUDd) is about 16.2oC, ranging from 14.9 ± 2.92oC, in Venezia to 17.4 ± 1.52oC, in Chioggia. The average humidity (URDd) of the municipalities is rather high with an average of 96.5% and the annual variation of about 1.6%. The minimum humidity

(URmin) is about  $18 \pm 4\%$  among the municipalities, whereas, in Venezia, the minimum humidity is significantly lower ( $13.9 \pm 3.8\%$ ). The number of days in a year with severe physical discomfort due to combined heat and high humidity (HuxWF) are about nine for the study area, whereas there is a wide range of variation between the municipalities with the lowest days (five and six days in Eraclea and Caorle, respectively) and the ones with the highest days (twelve and fifteen days in Cavallino-Treporti and Venezia, respectively).

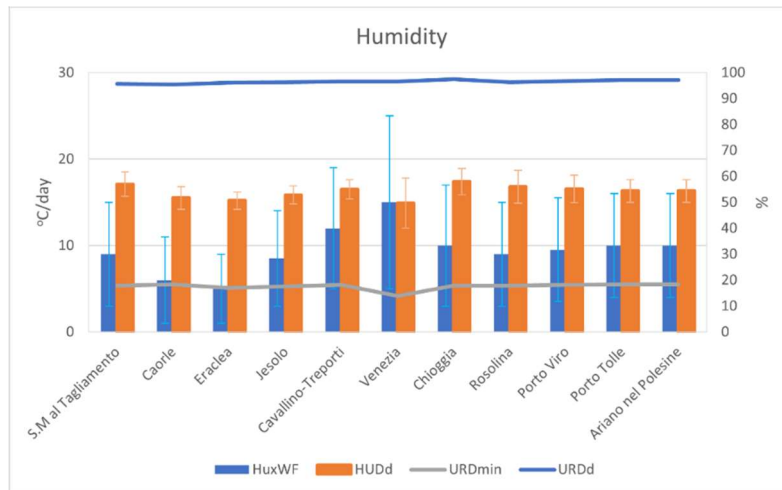


Figure 15. Humidity related indicators of eleven coastal municipalities averaged for the reference period 2009-2019. The blue columns represent number of days in year with severe physical discomfort due to combined heat and high humidity (HuxWF). The orange columns represent the humidex in Celsius degrees (HUDd). The blue and grey lines are the mean and minimum humidity in %, respectively. The vertical thin bars are standard deviation of the indicators over the reference period.

### 3.1.4 Wind related indicators

Wind is the natural movement of air or other gases caused by differences in atmospheric pressure, occurring in a wide range of scales (Makarieva et al., 2013). Wind is one of the most critical factors contributing energy to the formation and change of the coast by driving ocean currents and generating waves, which regulate sediment exchange of the coast (Kenchington et al., 2012). Wind is one of the important drivers of coastal flooding and erosion, which cause damages to ecosystems, properties, and infrastructures of various sectors in the coastal zone. Wind velocity is recorded hourly in the investigated stations at 10 m, 5 m, or 2 m.

Average and maximum wind velocity for the period 2009-2019 of the 11 coastal municipalities are shown in Figure 16. Average wind velocity (V10Dd) of the study area is around 1.9 m/s whereas the maximum wind velocity (VRFDD) is higher in the southern municipalities. Venezia has the lowest wind velocity, with the average and the maximum of  $1.3 \pm 0.1$  and  $8.2 \pm 1.2$  m/s, respectively. On

the other hand, Rosolina has the highest wind velocity, with the average of  $2.9 \pm 0.1$  m/s and the maximum of  $18.2 \pm 2.5$  m/s.

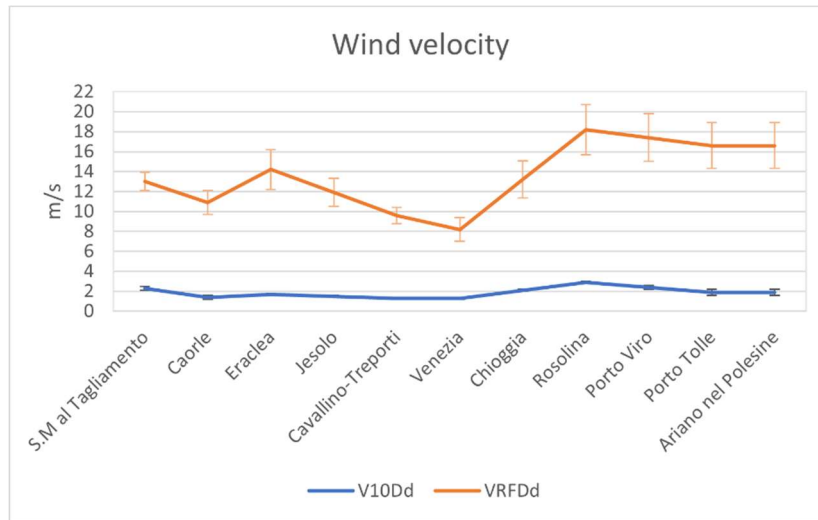


Figure 16. Wind indicators of 11 coastal municipalities averaged for the reference period 2009-2019. The blue line represents average wind velocity (V10d), while the orange line is the maximum wind velocity (VRFDd). The vertical thin bars are standard deviation of the indicators over the reference period.

### 3.1.5 Solar radiation

Solar radiation (RADd) is energy emitted by the sun in the form of electromagnetic radiation, a fundamental driver of the climate system on the Earth and a source for the energy sector. Changes in the frequency composition and intensity of incident solar radiation may cause changes in global and regional climate (Budyko, 1969), which contribute to heat up the Earth, causing sea level rise and increasing the frequency of more violent global weather patterns<sup>1</sup>.

The annual average solar radiation (RADd) of the 11 municipalities for the period 2009-2019 is shown in Figure 17. The RADd is about  $3,941.4 \pm 153.8$  W/(m<sup>2</sup>year) on average for the municipalities, whereas Caorle and Chioggia have lower values in solar radiation, which is of  $3,818.7 \pm 132.3$  and  $3,874.6 \pm 171.3$  W/(m<sup>2</sup>year), respectively. In general, the municipalities in the south tend to have higher solar radiation than the northern municipalities. Looking more details at the seasonal trend, solar radiation distributes similarly among the municipalities in winter. However, in the summer months, there is a high spatial variation, where solar radiation of the southern municipalities is especially higher than that in the northern ones. In fact, this trend can be explained

<sup>1</sup> [https://www.nasa.gov/topics/solarsystem/features/solar\\_variability.html](https://www.nasa.gov/topics/solarsystem/features/solar_variability.html)



by the distribution of precipitation, which is observed to be higher in the north (Figure 14a), where eventually less sunshine is recorded.

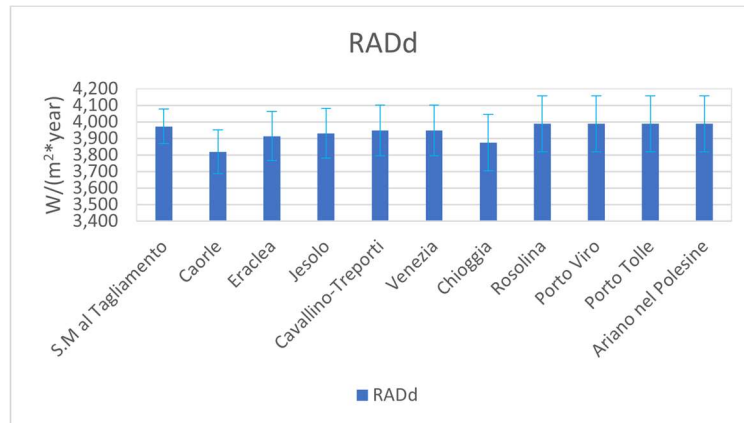


Figure 17. Solar radiation indicators of 11 coastal municipalities averaged for the reference period 2009-2019. The blue bars represent yearly average solar radiation (RADd). The vertical thin bars are standard deviation of the indicator over the reference period.

### 3.1.6 Atmospheric indicators calculated from the regional reanalysis data

To develop the Machine Learning approach for climate risk assessment in coastal areas of the Veneto Region (Deliverable 5.4.5), atmospheric indicators were calculated in parallel from ARPAV observed data (Section 3.1) and reanalysis datasets of the Copernicus Climate Data Store<sup>2</sup>. This section compares the distributions of ARPAV and reanalysis data, in order to understand the differences between the two databases.

The Copernicus Data Store contains, among others, two databases used in this application: The Uncertainties in Ensembles of Regional Reanalysis (UERRA; Ridal et al., 2017) and the Copernicus European Regional Reanalysis (CERRA; Schimanke et al., 2021). UERRA and CERRA are reanalysis products that provide gridded data built upon the combination of satellite observations, ground-based measurements and models' output of numerical weather prediction. They are parts of the two-phase service from the Copernicus Climate Change, which provides a long time series and high-resolution climate data for emergency response and disaster management in the European Union. UERRA database is the product of the first phase, the lateral boundary conditions used to constrain the model are extracted from ERA-Interim, including the UERRA-HARMONIE (11 km resolution; Jan 1961 - Jul 2019) and the MESCAN-SURFEX (5.5 km; resolution Jan 1961 - May 2019). CERRA dataset is the product of the second phase forced by the global ERA5 reanalysis (lateral boundary conditions), using as inputs a comprehensive combination of in-situ observations and satellite data that improves quality and is generally consistent over time. CERRA is more sophisticated than

<sup>2</sup> <https://cds.climate.copernicus.eu>

UERRA and includes more data assimilation from observations, particularly remote sensing data. This product is available at 5.5 km resolution from 1984 to the present.

The UERRA database was used for the bias-correction of the AdriaClim Atmospheric Model WRF (described in Deliverable D3.2.2), the products of which were then used as input for the Machine Learning methodology for the climate risk assessment detailed in Deliverable D5.4.5. It is necessary that the modelled data have a similar distribution to the dataset used to train and test the algorithm. Therefore, the Machine Learning algorithms were developed using reanalysis data. CERRA database was considered, given that the UERRA dataset does not cover the whole temporal range of the application (2009-2019). It is important to understand the similarities and differences between the CERRA data and the ARPAV data, as the latter contains information on the weather conditions registered on the days of interest.

**Figure 18** shows the comparisons of temperature, wind speed and precipitation indicators from the ARPAV and the CERRA datasets over the 11 coastal municipalities of the Veneto Region within the reference timeframe.

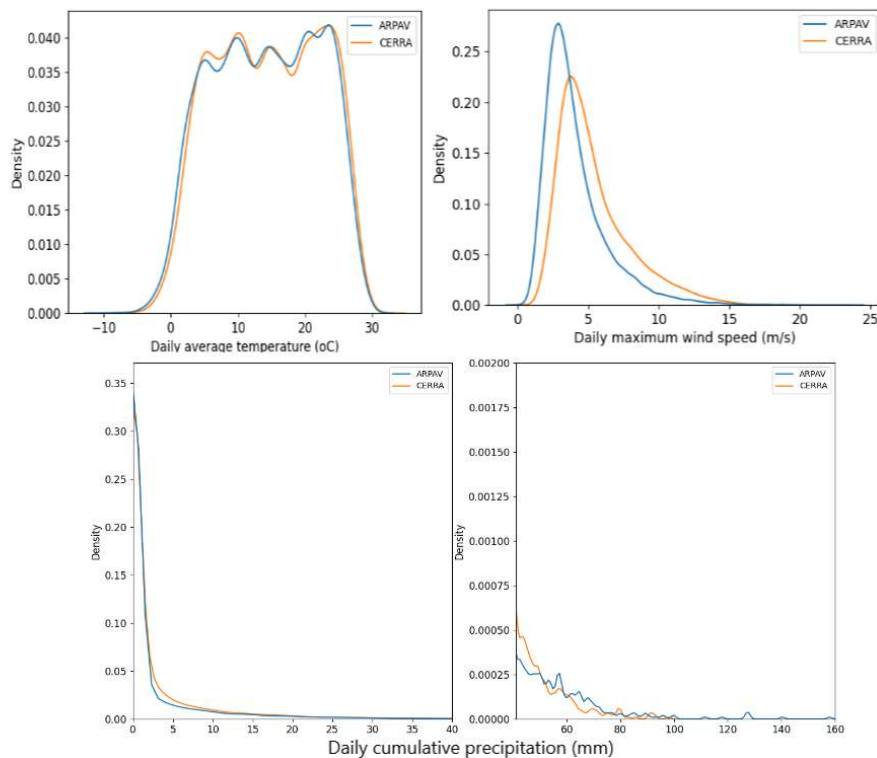


*Figure 18: Distributional comparison of the daily average temperature (top left), daily maximum wind speed (top right), and daily cumulative precipitation (bottom left – precipitation 0-40mm; bottom right 0 precipitation > 40mm) from ARPAV (blue line) and CERRA (orange line) datasets.*

There is a good agreement between the distributions of the daily average temperature from the two datasets (**Figure 18**, top left), which includes the tails of the curves, meaning that the number of days with extreme temperatures is similar in both datasets.

The daily maximum wind speed (**Figure 18**, top right) from CERRA shifts rightward compared to the ARPAV data, indicating that on average, the wind speed estimated by CERRA is higher than the wind speed estimated by ARPAV. In particular, the average value of daily wind speed for the 11 coastal municipalities of the Veneto region over the baseline timeframe (2009-2019) was 5.4 m/s if recorded from the CERRA, and 4.1 m/s from ARPAV.

The distributions of daily cumulative precipitation are similar in the two datasets (**Figure 18**, bottom). However, extreme precipitation values of more than 100 mm/day were recorded in ARPAV data, while CERRA could not detect such information.

Despite certain levels of discrepancies, similar distributions were found in the distributions of the atmospheric indicators between the ARPAV and CERRA datasets for the coastal municipalities of the Veneto Region. This would facilitate the analysis of climatic patterns along the case study with the high spatio-temporal resolution data spanning over a long-term period (1984 - present).

### 3.2 Marine indicators

Oceanographic characteristics play an important role in determining coastal hazards, i.e., coastal inundation, storm surge, saltwater intrusion, and erosion. Within the scope of this study, three important characteristics of ocean dynamic are considered: (i) sea level; (ii) ocean currents; and (iii) wave regimes. Sea level has a strong correlation with coastal inundation and seawater intrusion. The increase in tidal range and wave height in the surf zones, as well as the evolution of storm surges may be triggered by higher mean sea levels (Seneviratne et al., 2012). Meanwhile, sea level rise is the main factor increasing the occurrence of extreme sea levels. Ocean currents, on the other hand, are critically linked to global weather patterns related to the transport of heat and nutrients. Changes in ocean currents may lead to extreme heat events, intensified hurricanes, and enhanced sea level rise (Yin & Zhao, 2021; Zhang & Delworth, 2007). Wave regimes play a significant role in coastline formation and coastal floods. Coastal population, maritime activities, coastal and marine infrastructures are subjected to the impacts of severe waves waves (Seneviratne et al., 2012). Oceanographic variables for the Veneto pilot are collected from Copernicus Marine Service

(CMEMS)<sup>3</sup> from the European Union's Earth Observation Programme. The Copernicus Marine Service provides free-access, regular, and systematic reference information, variability and dynamic on physical, sea ice and biogeochemical state across global ocean and European regional seas. For the above-mentioned variables, we use the Mediterranean Sea Physics (Med-Physics)<sup>4</sup> and Sea Wave (Med-waves)<sup>5</sup> Reanalysis products. The Med-Physics is a product of a numerical composed hydrodynamic model, supplied by the Nucleus for European Modelling of the Ocean (NEMO) and a variational data assimilation scheme (OceanVAR). The Med-waves product is generated by the wave model WAM 4.6.2, which is a nested sequence of coarse and fine computational grids to ensure correct swell propagation from the North Atlantic towards the strait of Gibraltar into the Mediterranean Sea. The Med-Physics reanalysis is forced by hourly ECMWF ERA5 atmospheric forcing fields and assimilates reprocessed data, while the Med-waves is forced with daily averaged currents from Med-Physics and ECMWF ERA5 reanalysis 10m-above-sea-surface winds. Both products have a regular grid of  $1/24^\circ$  (ca. 4-5 km) covering the Mediterranean Sea. The Med-waves has hourly temporal resolution covering from 1993, while the Med-Physics expands from 1987 with mean hourly, daily, and monthly resolutions.

The datasets are provided in NetCDF format. The daily mean and/or maximum value of the selected variables were calculated and assigned to each municipality in QGIS and Python platforms. Altimetric parameters related to sea surface and wind wave heights were converted to local datum. Acqua Alta Platform<sup>6</sup> was considered as reference monitoring station to perform the conversion with baseline period from 1991-2020. The mean difference in observed and modelled was computed and add to the model dataset over the whole domain. Total current velocity was calculated as the vector sum of the norward and eastward sea water velocity. For wave regime, given the similarity between wave and wind wave parameters in the north Adriatic Sea, only wind wave parameters were selected to report to avoid duplications. Wind wave direction (WID) at maximum wind wave height (MWH) was extracted to capture extremity of the events.

### 3.2.1 Sea level

The average value of daily mean sea surface height (SSH) of the Veneto coastal water for 2009-2019 is about  $0.32 \pm 0.13$  m, with a variation from -0.27 m to 0.98 m. As observed from Figure 19a, there is a slight increase in SSH from north to south. In particular, average SSH slightly ranges from  $0.30 \pm 0.13$  m (San Michele al Tagliamento) to  $0.34 \pm 0.13$  m (Ariano nel Polesine). Daily time series of SSH

---

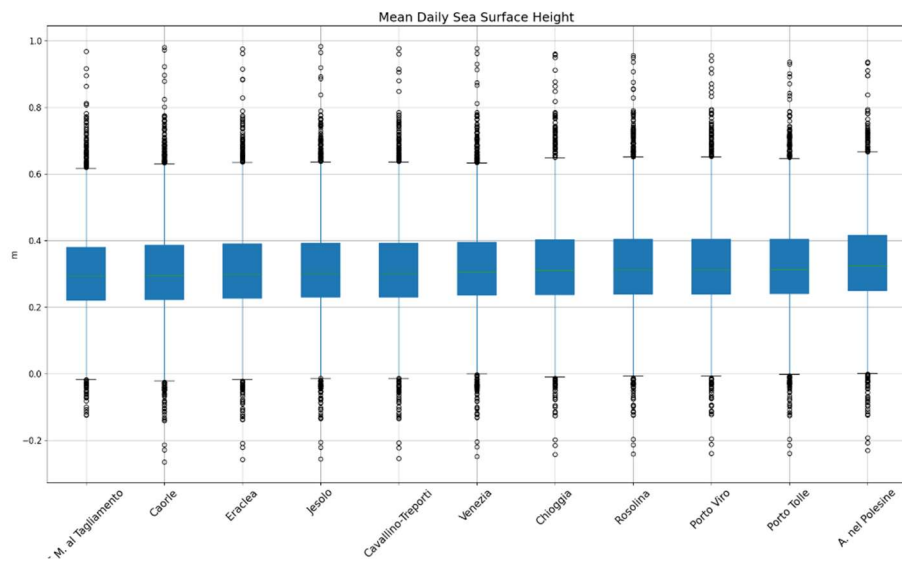
<sup>3</sup> <https://marine.copernicus.eu/>

<sup>4</sup> [https://resources.marine.copernicus.eu/product-detail/MEDSEA\\_MULTIYEAR\\_PHY\\_006\\_004/INFORMATION](https://resources.marine.copernicus.eu/product-detail/MEDSEA_MULTIYEAR_PHY_006_004/INFORMATION)

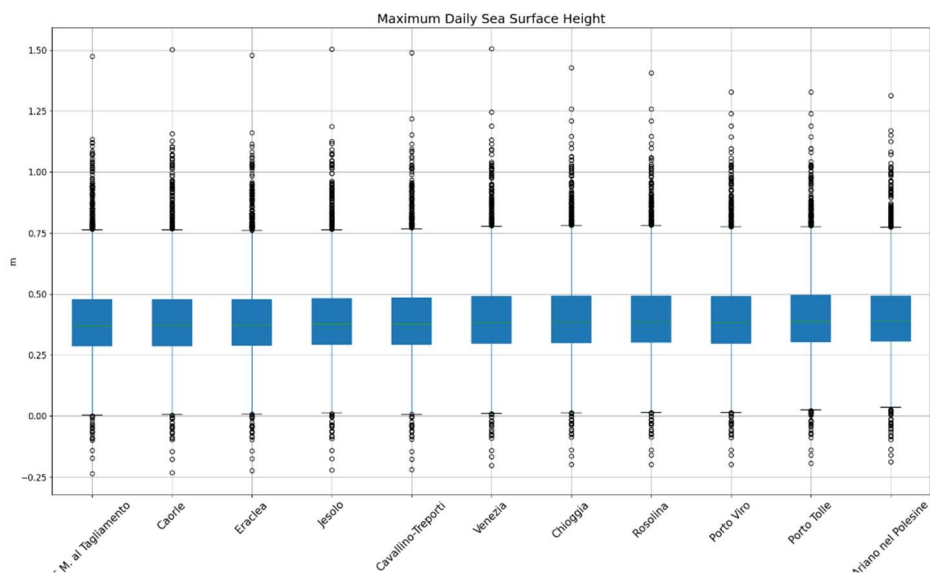
<sup>5</sup> [https://resources.marine.copernicus.eu/product-detail/MEDSEA\\_MULTIYEAR\\_WAV\\_006\\_012/INFORMATION](https://resources.marine.copernicus.eu/product-detail/MEDSEA_MULTIYEAR_WAV_006_012/INFORMATION)

<sup>6</sup> [http://www.ismar.cnr.it/infrastructures/piattaforma-acqua-alta?set\\_language=en&cl=en](http://www.ismar.cnr.it/infrastructures/piattaforma-acqua-alta?set_language=en&cl=en)

for the coastal waters of Veneto region does not show a clear trend of increasing in sea level. Similarly, MSSH distributes with a slight increase southward (Figure 19b). Lowest MSSH is found in San Michele al Tagliamento ( $0.39 \pm 0.16$  m) while Ariano nel Polesine gets the highest MSSH recorded ( $0.41 \pm 0.16$  m). Average MSSH for the whole Veneto coastal waters is approximately  $0.4 \pm 0.16$  m with extreme values might be found up to 1.51 m. At a height of 1.10 m of sea surface, it is worth noting that about 12% of the Venice city is flooded (Ferrarin et al., 2019). Therefore, extreme SSH is among the concerns for coastal inundation.



(a)



(b)

Figure 19. Boxplots at municipality level of daily mean (a) and maximum (b) sea surface height in the Veneto coastal water (2009-2019).

### 3.2.2 Ocean current velocity

Mean daily current velocity of the Veneto coastal water for 2009-2019 is  $0.098 \pm 0.046$  m/s, with minimum and maximum values are found at 0.015 m/s and 0.391 m/s, respectively (Figure 20). Due to geographical characteristics with a curved coastline, municipalities located in the concave central coast have lowest current velocity ( $0.038 \pm 0.007$  m/s) compared to these in the north ( $0.049 \pm 0.012$  m/s) and the south ( $0.056 \pm 0.022$  m/s). Notably, Porto Tolle has significant higher values of current velocity caused from its extreme convex location of the coastline. In particular, average current velocity of Porto Tolle is  $0.19 \pm 0.087$  m/s with maximum values ranging up to 0.683 m/s.

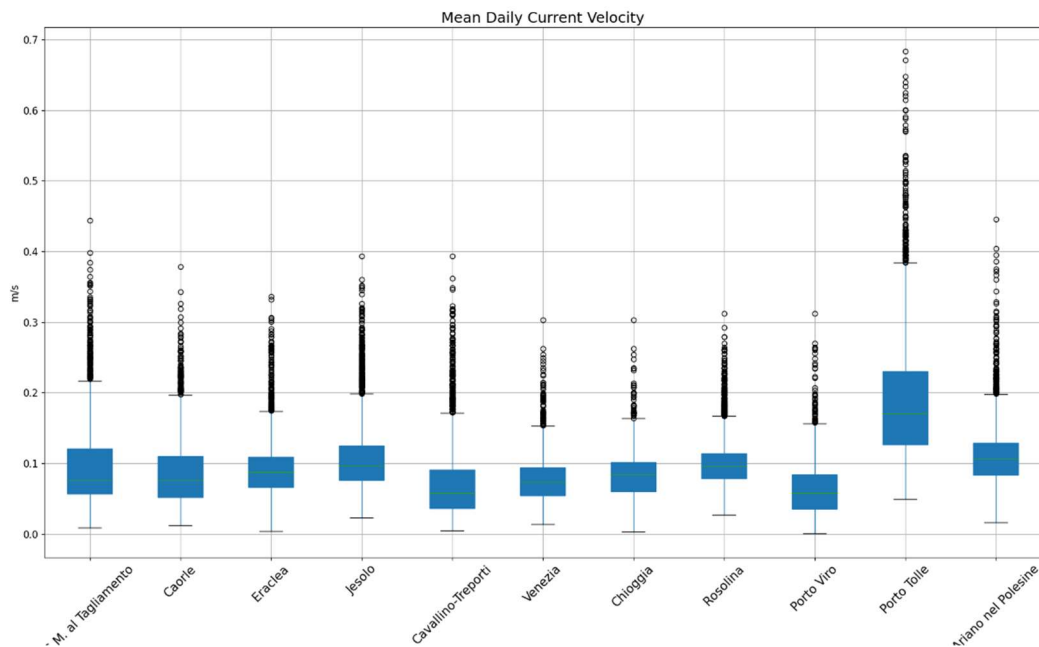


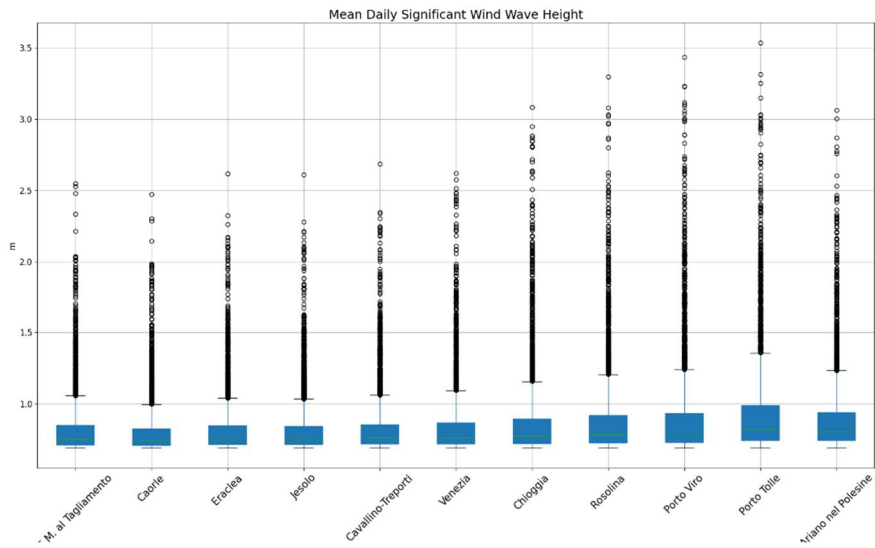
Figure 20. Boxplots at municipality level of daily water velocity in the Veneto coastal water (2009-2019).

### 3.2.3 Wave regimes

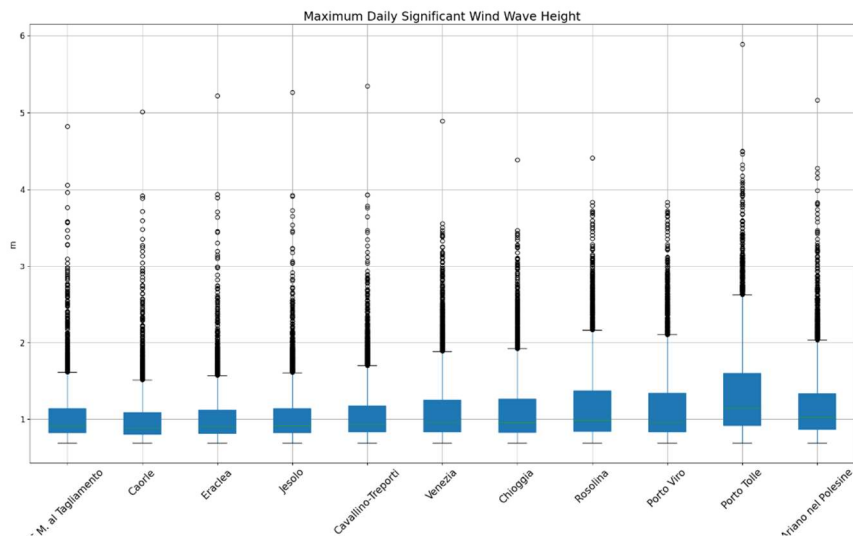
#### Significant wind wave height

Significant wave height is among the metrics of marine storm intensity and its potential damages (Lionello et al., 2012). WIH of the Veneto coastal water for the period 2009-2019 ranges from 0.69 m to 2.9 m, with daily average value recorded at  $0.87 \pm 0.25$  m (Figure 21). WIH slightly increases

from north to south and reaches its peak in Porto Tolle (average  $0.94 \pm 0.26$  m), where extreme value can be found at 3.5 m. Maximum daily WIH shows a similar trend with average values increase southward. However, MWIH shows a significant higher magnitude with an average of  $1.12 \pm 0.44$  m, minimum of 0.69 m, and maximum at 5.87 m.



(a)



(b)

Figure 21. Boxplots at municipality level of daily mean (a) and maximum (b) significant wind wave height in the Veneto coastal water (2009-2019).

### Wind-wave mean period

Wind wave in the Veneto coastal water has an average period of  $1.50 \pm 0.62$  s with minimum and maximum values of 0.99 s and 5.02 s, respectively (Figure 22). Southern coastline is exposed to higher wind wave period with a peak at Porto Tolle (average  $1.70 \pm 0.75$ s) meanwhile extreme value reaches its peak in Ariano nel Polesine (maximum 5.68 s).

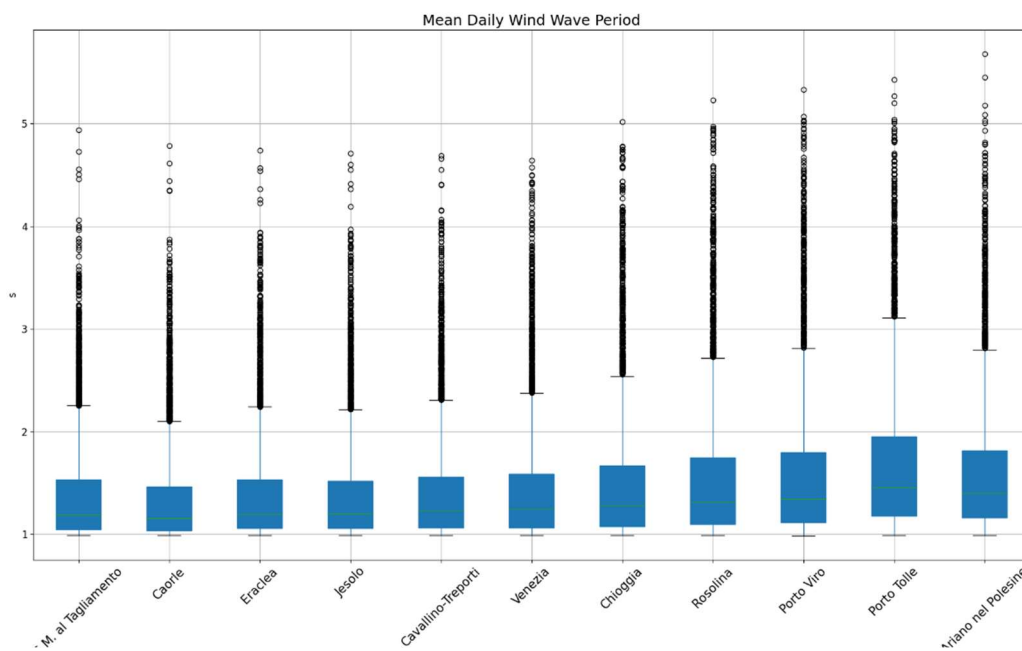


Figure 22. Boxplots at municipality level of daily average wind wave period in the Veneto coastal water (2009-2019).

### Wind wave direction at maximum wind wave height

Wave direction recorded at maximum wind wave height is shown in Figure 23 by its density of distribution. Based on geological characteristics and direction of the coast, wind wave direction approach the municipality with 3 distinguished groups: (i) San Michele al Tagliamento and Caorle with most frequent direction of wind wave range from 160o to 200o; (ii) Eraclea, Jesolo, Cavallino-Treporti, Venezia, and Chioggia with a flatter peak distributed from 100o to 200o; and (iii) Rosolina, Porto Viro, Porto Tolle, and Ariano nel Polesine with wind wave direction mostly distribute from 120o to 210o.



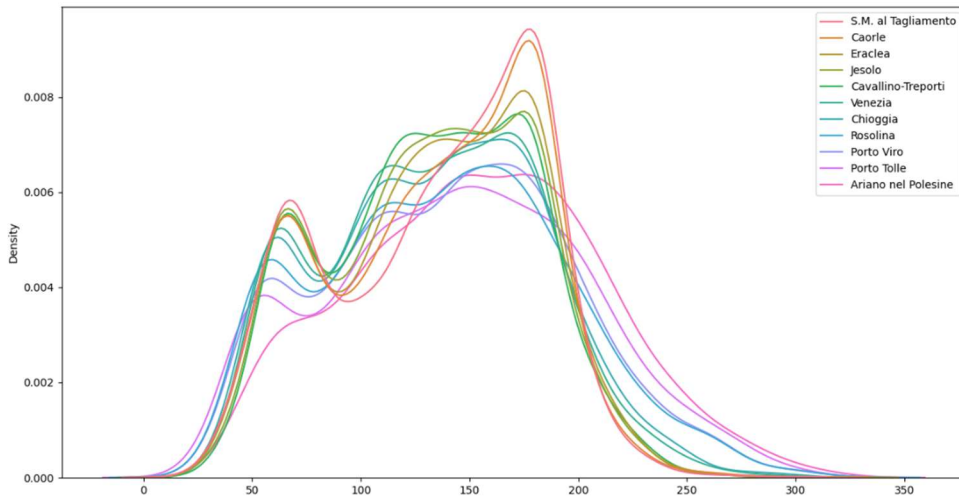


Figure 23. Density distribution of wind wave direction at maximum wind wave height in Veneto coastal water (2009-2019).

### 3.3 Territorial indicators

This section covers territorial characteristics of the coastal municipalities of the Veneto Region, including a very large set of indicators of different typologies and attributes. The common linkage within these data is that they provide information of the territorial characteristics, such as geomorphology, topology, coastal defense magnitude, etc. These indicators play an important role in multi-risk assessment as they are considered as triggering/contributing factors to determine climate related impacts, or as exposure and vulnerability.

#### 3.3.1 Land use indicators

Land use indicators reports the relative surface area (%) of the territory covered by general use typology (i.e., clusters), including Anthropic, Agriculture/fisheries, Natural, Beach, Internal water and Other, respect with to the total surface area of the considered municipality.

Figure 24 reports the values of each indicator for each municipality and in relation to the 4 different datasets (2006, 2012, 2015 and 2018), whereas Figure 25 shows the associated thematic maps. Analyzing the values, several observations can be deduced by the annual scores of each indicator, such as their changes within the 4 different datasets.

The indicator Anthropic land use has homogeneously similar values within all the municipalities, showing values of about 10-15%. The only exceptions are within the municipality of Venice, Cavallino-Treporti and Jesolo, whose value is between 20% and 30%, and consequently result the

most relatively anthropized municipalities. Overall, this indicator shows a clear trend within the 4 datasets, displaying an increasing of 3-4% between 2006-2018, except for Rosolina and Venice, where this indicator slightly decreased of 1-2% within the same period.

The indicator Agriculture/fisheries is always the most abundant within all the municipalities, with values ranging between 48% and 92%, with the exception of Venice whose values is about 22-25%. This indicator is quite stable within the 4 datasets, displaying a significant variation (about 5%) only in Caorle (decrease), Rosolina (increase) and Cavallino-Treporti (decrease) between 2006-2018.

The indicator Natural shows important different values within the 11 considered municipalities, since it ranges between 1% to 16%. Overall, Rosolina and Chioggia are the municipalities with the higher values, whereas Eraclea has the minimum score. The values of this indicator are extremely stable within the 4 datasets and the changes never exceeds the 1-2% in each municipality between 2006-2018.

The indicator Beach present values very low in the scoring of land use coverage. The values are generally between the 0.5% and 1.5% for each municipality, and the changes within the 4 datasets are very minimal (except for Cavallino-Treporti which shows an increasing of 3% in the period 2006-2018). However, since the detection of beaches in the land use definition process is quite difficult because they occupy a narrow long area of the territory, and since a small difference in the spatial cover domain is revealed within the 4 datasets (consequently in some municipality/year beaches were not mapped in the land use datasets), the changes of this indicator values are considered neglectable.

The indicator Internal water shows an extremely high variance within the 11 considered municipalities, since it ranges between 1% to the 44%. Overall, within the 11 municipalities, the values do not exceed the 10%, but with important exception for Porto Tolle (circa 25%), Rosolina (circa 15%), Chioggia (circa 24%) and especially Venice (circa 44%). The high value of this indicator in the Venice territory is related to the presence of the Venice Lagoon. Generally, a clear trend of change is not identifiable within the 4 different datasets, although slightly variations were observed within all the municipalities in the period 2006-2018, especially in Cavallino-Treporti and Carole (changes of about 3%).

The indicator Other does not show important values within the 11 municipalities and within the 4 datasets, and the values are always about the 0.2-0.5% with neglectable variations.

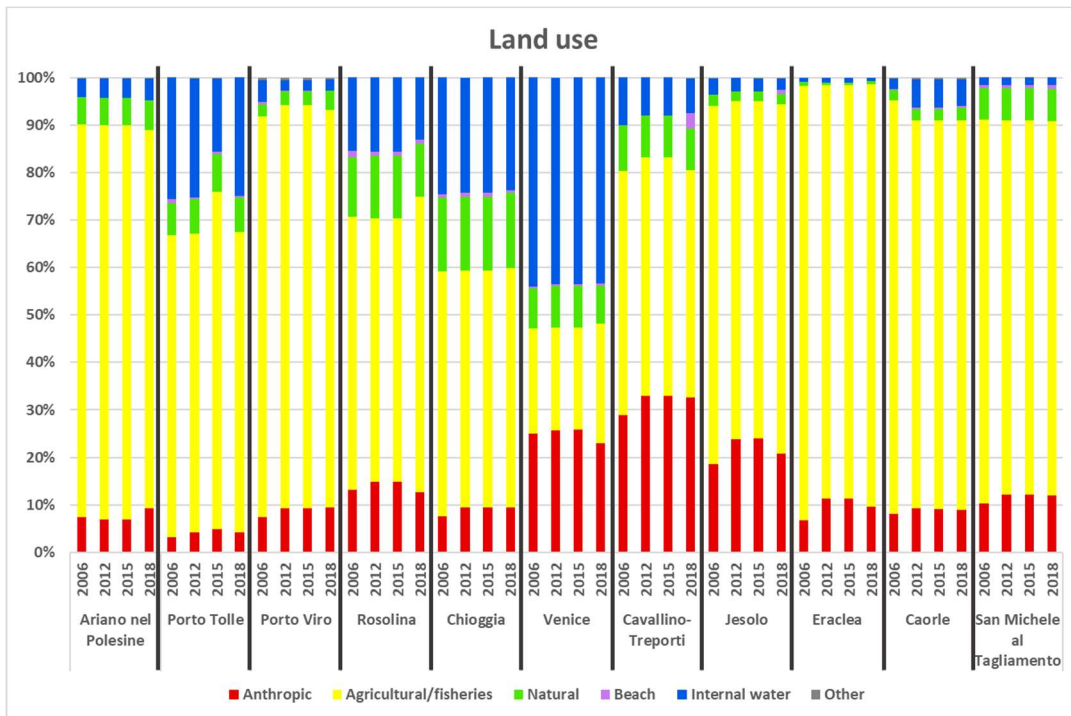


Figure 24. Land use indicator values for each municipality within the 4 datasets (2006, 2012, 2015 and 2018) available for the reference period.

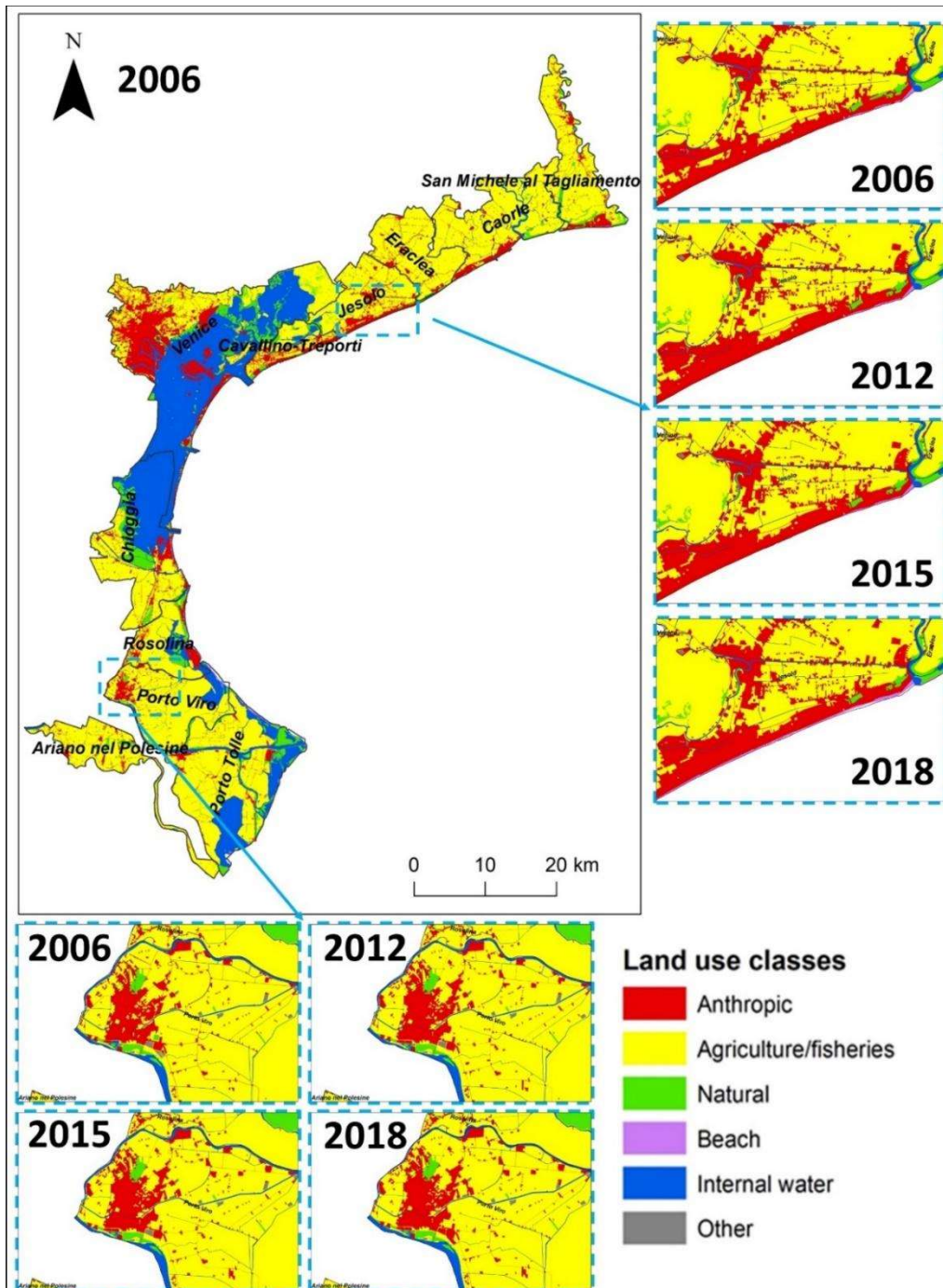


Figure 25. Land use indicators represent the distribution of land use classes within the 11 considered municipalities. The changes in the land use between the 4 datasets (2006, 2012, 2015 and 2018) are minimal, and they can be appreciated only in small high-zoomed areas. In the boxes, for example, is reported the expansion of the anthropic class (e.g., growing

*urban centres, construction of infrastructures, etc.) between the 4 datasets in correspondence of Jesolo and Porto Viro cities.*

### 3.3.2 Coastal protection on shoreline and dune indicators results

These indicators report the coastal length (absolute or relative) covered by coastal protections or dunes located on the shorelines on each municipality (e.g., beach, natural areas, river delta). In the Table 2 are reported the values of the two indicators on each municipality, whereas in the Figure 26 are reported the associated thematic maps.

Overall, the municipalities in the northern sector and within the administrative boundaries of the Metropolitan City of Venice (i.e., San Michele al Tagliamento, Caorle, Eraclea, Jesolo, Cavallino-Treporti, Venice and Chioggia) presents the larger length of coast covered by protections. In some cases, the coverage is close or equal to 100% (e.g., Eraclea, Jesolo and Cavallino-Treporti). Conversely, the municipalities within the Rovigo province (Rosolina, Porto Viro, Porto Tolle and Ariano nel Polesine), present a significant lower coastal length covered by shorelines' protections (i.e., between 13% to 30%). It must be noted that a major part of the coastal protections on beach is composed by groins ('pennelli') which main goal is enhancing sediment deposition and beach accretion. For this reason, their larger distribution on the northern municipality is explained by the major seaside touristic vocation of these territories, and consequently their needing to protect the beaches from erosion and to maintain a high quality of the touristic offer.

Considering the dunes indicator, it is observed the opposite trend: the southern municipalities have a higher coastal length with the presence of dunes (about the 54-65%, estimated as dune length/total length of shoreline). The only exception is represented by Ariano nel Polesine, which does not display dunes presence on its territory (however this can be explained by its significant smaller coastal length respect with to the other municipalities). Conversely, the municipalities within the Metropolitan City of Venice have a smaller coastal dune coverage (18-41%), with the only exception of Eraclea that shows a value of about 75%.

Moreover, where dunes are present the coastal protection are generally missing and vice versa, showing a complementary distribution. This can be related to two factors: i) southern municipalities show a less percentage of anthropogenic areas (i.e., anthropic and agricultural/fisheries land use classes) and present a minor anthropogenic pressure since historical times, and consequently they have the possibility to host larger natural habitats, including dune zones that are incompatible with human constructions ii) dunes act as natural protectors from coastal erosion and marine inundations, so the needing for built artificial structures to cope with these phenomena is probably not required on territories that host them. However, it must be highlighted that the territories within the Rovigo province (i.e., within the Po delta area) are significantly low respect the sea level, and consequently threatened; these territories are indeed protected by marine hazards from a diffuse net of artificial protections (e.g., walls, embankments) and pumping systems (e.g.,

dewatering). These solutions however are not located directly on the littoral areas, so they were not counted in the coastal protection dataset/layer (and in the indicator calculation).

Table 2. Coastal protection on shoreline and dune indicators values (absolute and relative) on each considered municipality for the reference scenario.

	Tot. length shoreline (km)	Coastal protection length (km)*	Ratio coastal protection (%)	Dune length (km)	Ratio dune (%)
<b>S.M. al Tagliamento</b>	10.34	8.18	79.19	2.91	28.15
<b>Caorle</b>	19.45	14.04	72.21	5.99	30.82
<b>Eraclea</b>	2.91	2.91	100.00	2.20	75.47
<b>Jesolo</b>	16.33	15.11	92.49	2.90	17.76
<b>Cavallino-Treporti</b>	18.75	17.24	91.93	7.76	41.36
<b>Venice</b>	31.36	27.29	87.04	11.89	37.91
<b>Chioggia</b>	10.35	7.81	75.47	4.00	38.65
<b>Rosolina</b>	14.35	4.37	30.46	7.72	53.82
<b>Porto Viro</b>	6.35	1.58	24.82	4.10	64.68
<b>Porto Tolle</b>	40.06	7.40	18.48	23.04	57.52
<b>Ariano nel Polesine</b>	1.41	0.19	13.19	0.00	0.00

\*Only defense protections placed along the shoreline (e.g., groins, jetties, breakwaters) were considered in the count.

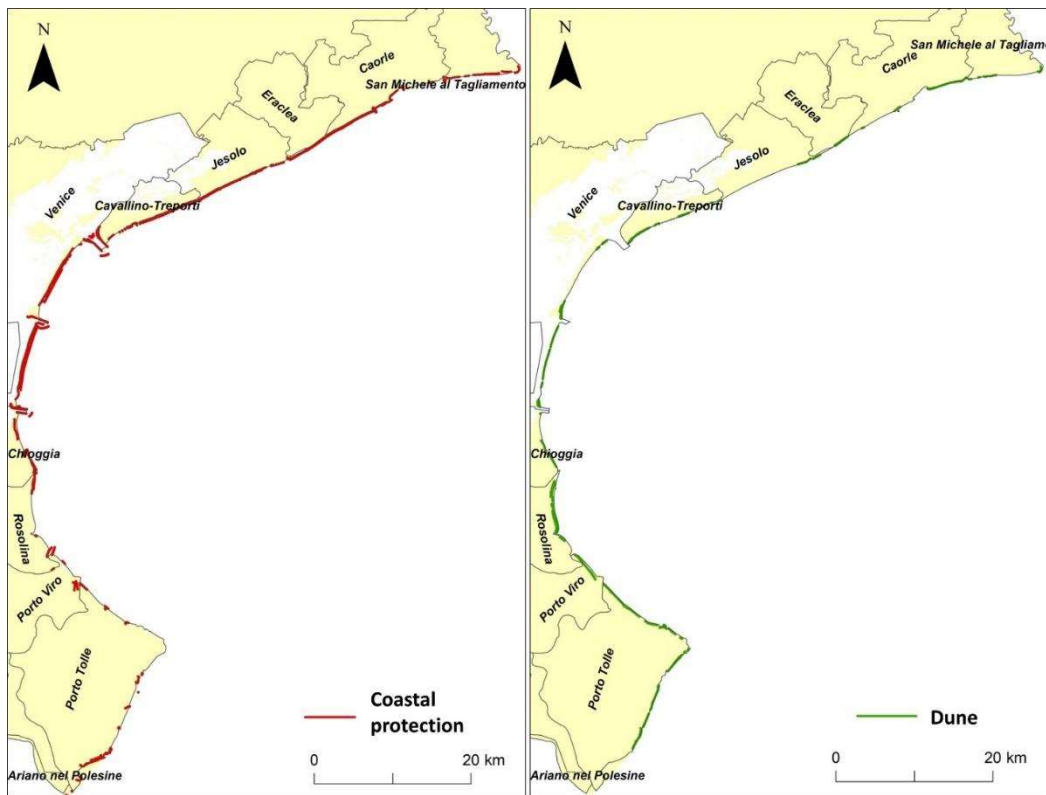


Figure 26. Coastal protection on shoreline and dune indicators representing the presence of coastal protections (on the left) and dunes (on the right) on the shorelines on the 11 considered municipalities in the reference period.

### 3.3.3 Subsidence

Subsidence is the vertical downward movement of the Earth's surface, which results from both natural and anthropogenic processes (J. A. Jackson, 2005). In coastal areas, land subsidence magnifies the local effect of climate change and sea-level rise (Erkens et al., 2015), increasing coastal flooding and inundation risks. Besides, land subsidence also affects urban drainage systems and causes damages and losses on properties of various sectors (Swiss Re, 2007).

Subsidence data of the coastal municipalities in Veneto is collected from the 'Geodatabase gestionale delle coste venete' (GCV - Progetto coste) for the period 2002-2010. Subsidence rate (mm/year) is classified into 5 classes: (1) <-10; (2) from -10 to -5; (3) from -5 to -2; (4) from -2 to 2; and (5) >2.

The integration of land subsidence in multi-risk assessment has been highlighted in the study of (Gallina et al., 2020). Land subsidence in Veneto region occurs at different extents. Whereas some areas are characterized with a relatively stable subsidence rate, and even the upward movement of

land, some areas of the Veneto region experience high subsidence rate with some hotspots identified in the inlets of the Venice Lagoon and the Po River Delta (Ruol et al., 2016). In order to evaluate the contribution of the subsidence rate within our risk assessment methodology, we focused on the areas with the downward subsidence rates higher than 2 mm/year (or in the other word, with the subsidence rate lower than -2 mm/year). Therefore, we selected the areas associated to class 1 (<-10 mm/year), class 2 (from -10 to -5 m/year), and class 3 (from -5 to -2 m/year). Zonal histogram plugin in QGIS was used to obtain the numbers of pixels of each of these classes for each municipality, which were then multiplied to the pixel size of 50 m x 50 m. Finally, the total area of the selected classes is divided with the total area of the municipality to attain the percentage of areas with a downward subsidence rate over - 2 mm/year of each municipality.

The risk assessment considers the total extent of areas with a downward subsidence rate higher than 2 mm/year (or in the other word, with a subsidence rate lower than -2 mm/year). This subsidence rate occurs in all the municipalities with different extensions, which accounts for more than 30% of all municipalities, except for Venezia, which accounts for 19.3% (Figure 27). Notably, Eraclea and Jesolo have more than 60% of area occurring downward subsidence with a subsidence rate more than -2 mm/year, whereas that of Cavallino-Treporti has a significantly high proportion of 91.9%.

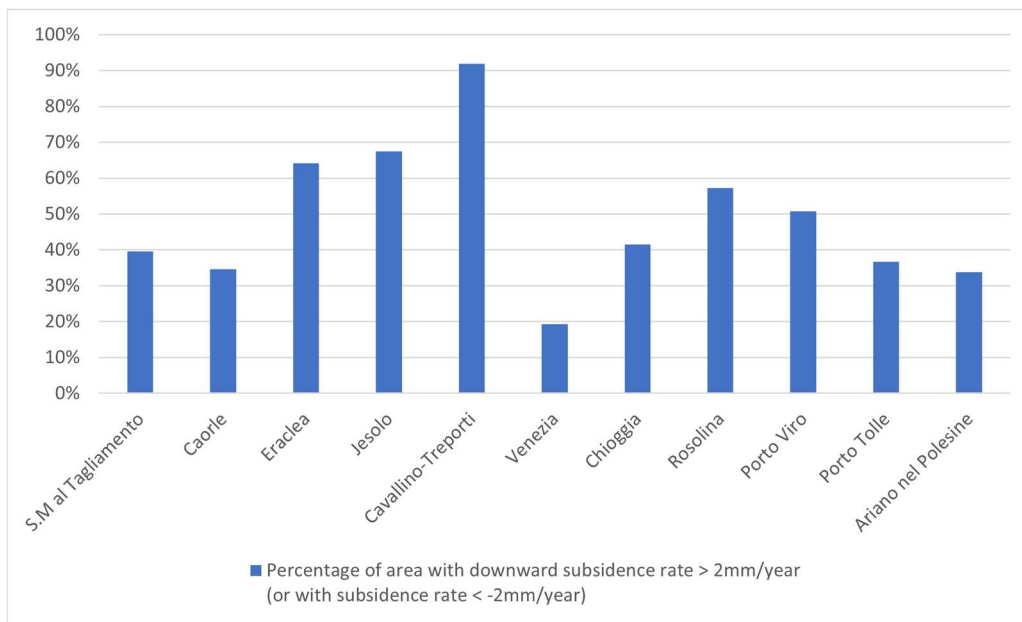


Figure 27. Subsidence indicators representing the percentage of area with a downward subsidence rate of more than 2 mm/year (or in the other word, with a subsidence rate lower than -2 mm/year) in the coastal municipalities of the Veneto region, for the reference period.



### 3.3.4 Topographic indicators

Topography is an important triggering factor to pluvial floods, coastal flooding, inundation, and erosion. Topographical characteristics of a receptor define their vulnerability level to coastal hazards (Torresan et al., 2012).

Topographical maps are derived directly from the Digital Elevation Model (DEM) of 10 m x 10 m obtained by the National Institute of Geophysics and Volcanology (INGV)<sup>7</sup>. The latest dataset available for the reference period with the spatial resolution over the Veneto region is in 2007. Given that the topographical characteristics of an area changes at a low rate (Conrad & Husson, 2009), and within the reference period, they are considered constant. Therefore, the use of DEM in 2007 is suitable for the risk assessment in the reference period. From DEM, the Terrain Analysis tool was used in the System for Automated Geoscientific Analyses (SAGA) program to produce maps of slope, aspect, plan curvature, ruggedness of the study area according to the second order polynomial method of (Zevenbergen & Thorne, 1987). Then, the average and standard deviation of each parameter for each municipality were calculated using the Zonal Statistics tool in QGIS and used as input for the model.

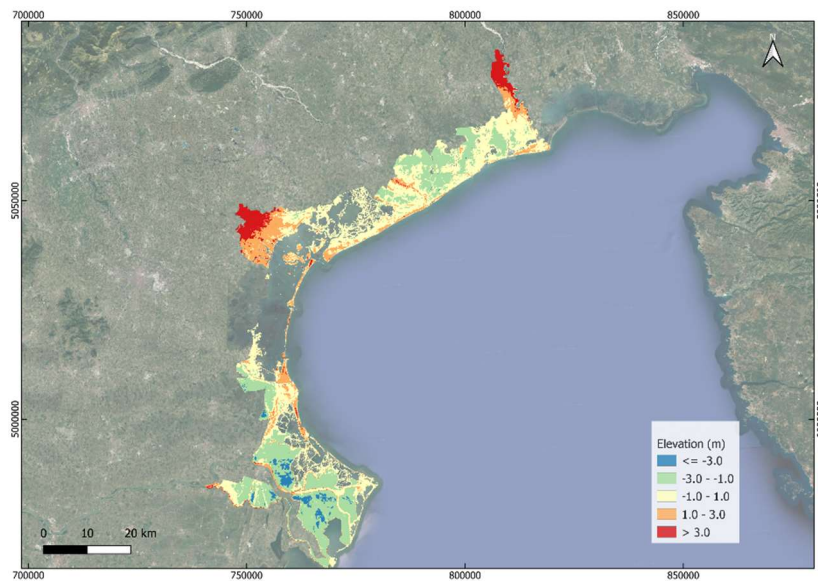
Table 2 shows the topographic indicators of the study area with average and standard deviation values at municipality level. The municipalities are generally characterised by low plain terrain with low elevation, slope, and ruggedness index (RI), as depicted in Figure 28. The average elevation ranges from  $-1.19 \pm 1.38$  m (Porto Tolle) to  $1.75 \pm 2.73$  m (S.M. al Tagliamento). The terrain in the study area is homogenous with low RI values, which ranges from  $0.02 \pm 0.03$  m (Cavallino-Treporti) to  $0.09 \pm 0.19$  m (Ariano nel Polesine). The study area is relatively flat (nearly level), with the average slope ranging from  $0.18 \pm 0.25$ o (Cavallino-Treporti) to  $0.66 \pm 1.44$ o (Ariano nel Polesine). Most of the municipalities have convex-majority slopes with positive plan curvature values, except for Eraclea, which has a negative plan curvature value.

*Table 2. Topographic indicators calculated for the coastal municipalities of the Veneto Region in the reference scenario.*

Municipalities	Average elevation (m)	Average slope (o)	Average aspect (o)	Average plan curvature	Average RI (m)
<b>San Michele al Tagliamento</b>	$1.75 \pm 2.73$	$0.31 \pm 0.52$	$187 \pm 99$	$0.0005 \pm 0.09$	$0.04 \pm 0.07$
<b>Caorle</b>	$-0.77 \pm 0.85$	$0.24 \pm 0.30$	$182 \pm 103$	$0.0005 \pm 0.12$	$0.03 \pm 0.04$

<sup>7</sup> <http://tinitaly.pi.ingv.it/>

Municipalities	Average elevation (m)	Average slope (o)	Average aspect (o)	Average plan curvature	Average RI (m)
<b>Eraclea</b>	-0.79±1.02	0.32±0.59	178±107	-0.0002±0.13	0.04±0.08
<b>Jesolo</b>	-0.02±0.93	0.39±0.68	187±102	0.0045±1.76	0.05±0.09
<b>Cavallino-Treporti</b>	0.54±0.54	0.18±0.25	188±108	0.0048±0.16	0.02±0.03
<b>Venezia</b>	0.87±1.6	0.22±0.61	176±102	0.0027±0.19	0.03±0.08
<b>Chioggia</b>	-0.18±1.08	0.20±0.47	181±102	0.0012±0.14	0.03±0.06
<b>Rosolina</b>	0.15±0.93	0.31±0.62	177±103	0.0052±0.23	0.04±0.08
<b>Porto Viro</b>	-1.03±1.47	0.31±0.94	178±98	0.0034±0.26	0.04±0.12
<b>Porto Tolle</b>	-1.19±1.38	0.35±1.07	177±103	0.0022±0.4	0.05±0.14
<b>Ariano nel Polesine</b>	-0.96±1.64	0.66±1.44	168±104	0.0011±0.15	0.09±0.19



(a)

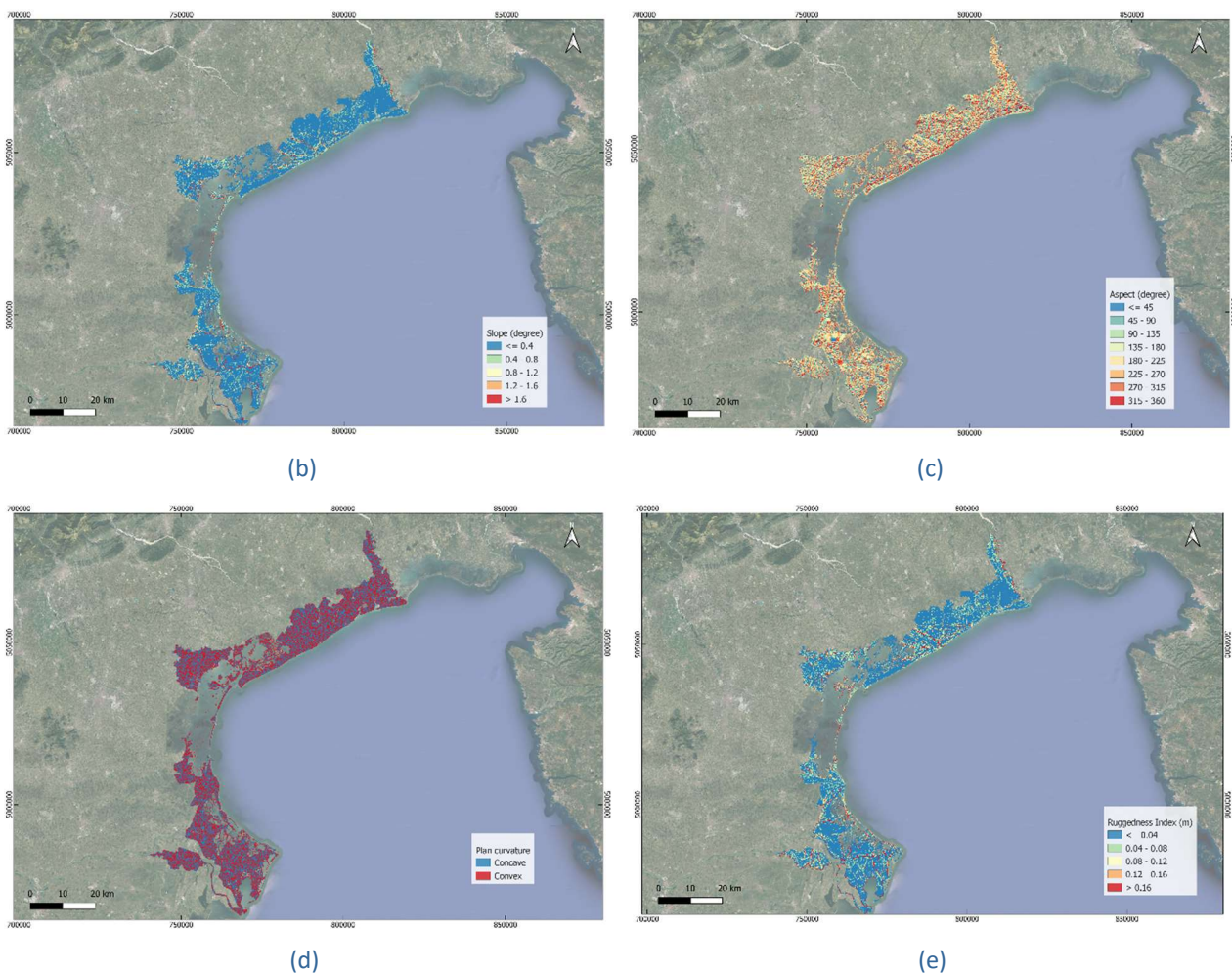


Figure 28. Topographic indicators calculated for the coastal municipalities in the Veneto region for the reference period: (a) elevation; (b) slope; (c) aspect; (c) plan curvature; and (d) ruggedness index.

### 3.3.5 Soil types

Soil type is an essential indicator of vulnerability and sensitivity of a receptor to coastal hazards. Soil characteristics such as texture and permeability level directly affect the drainage process and stability of a surface, which play a significant role in assessing risks from pluvial floods, coastal flooding, inundation, and erosion (Mojaddadi et al., 2017; Torresan, Critto, Rizzi, & Marcomini, 2012).

For the assessment of risks in the Veneto pilot, the classification of soil indicator distinguished only 2 soil types based on their sensitivity to coastal hazards, which include: CL1 - Soils on dune ridges and lagoon islands, formed by sands, from very to extremely calcareous and CL2 - Soils on reclaimed

lagoon areas, artificially drained, formed by very to extremely calcareous silts. In fact, sandy beaches and artificial drainage lagoons are considered more vulnerable to storm surges and coastal erosion (Gallina et al., 2019; Torresan et al., 2012, 2008). The extent of these 2 classes over a municipality is calculated based on the ratio between the total area of each class and the municipality's total area. The study area is characterized by 11 soil classes, as depicted in Figure 29.

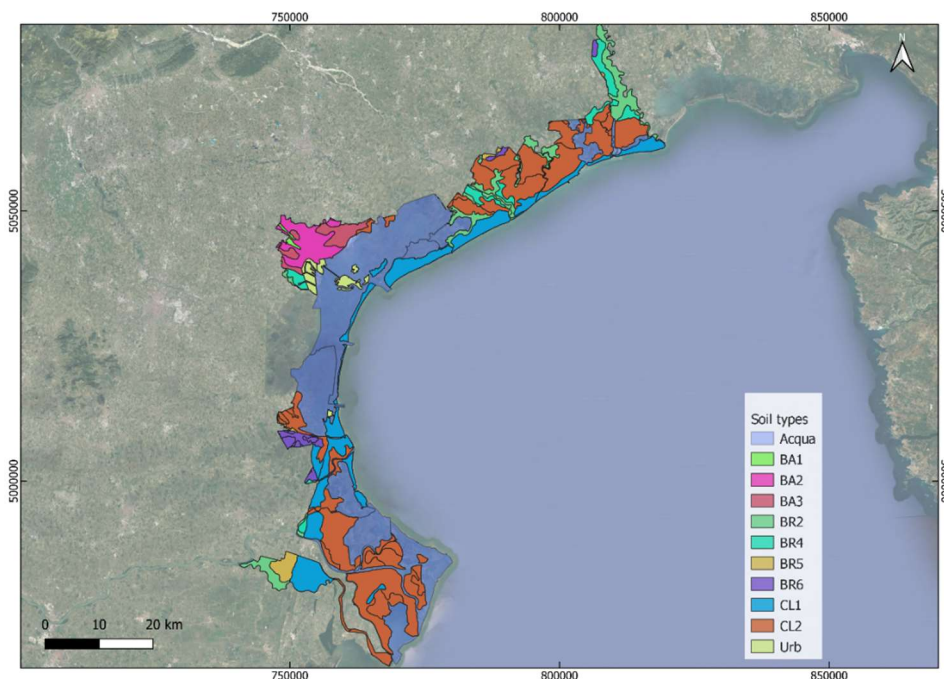


Figure 29. Soil indicator extracted for the coastal municipalities in the Veneto Region for the reference period.

The extent of CL1 (Soils on dune ridges and lagoon islands, formed by sands, from very to extremely calcareous) and CL2 (Soils on reclaimed lagoon areas, artificially drained, formed by very to extremely calcareous silts) classes in the municipalities is shown in Figure 30. There is an uneven distribution of the two classes in the municipalities. CL1 distributes in the whole study area. Cavallino-Treporti and Ariano nel Polesine have a significant proportion of 64.2% and 41.3%, respectively, whereas, in some municipalities, CL1 accounts for a low proportion, namely Porto Tolle and Venezia, of 1.1% and 3.2%, respectively. On the other hand, CL2 presents in most municipalities, except for Cavallino-Treporti. CL2 distributes predominantly in some municipalities, such as Porto Tolle, Caorle, and Eraclea, with a proportion of up to 66.8%, whereas in Venezia, its distribution is relatively low (1.3%).

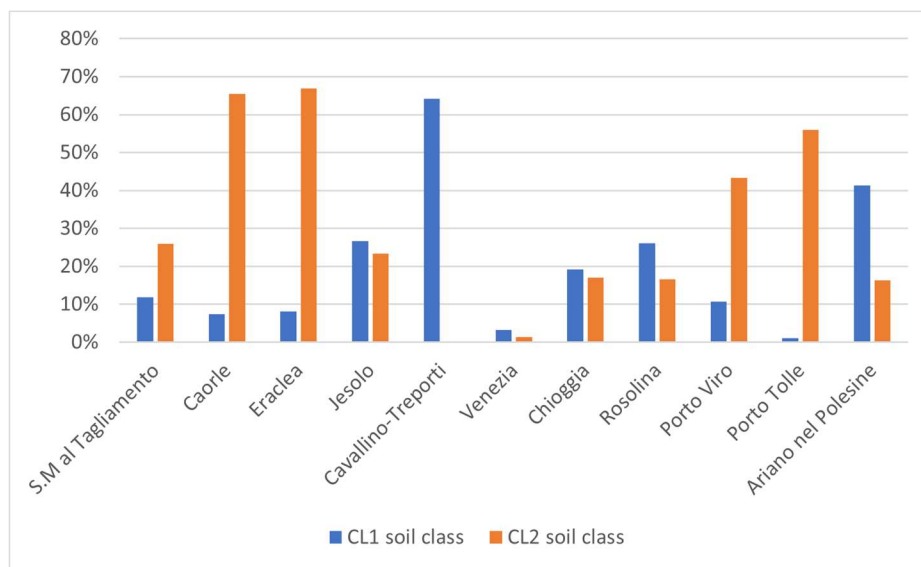


Figure 30. Percentage of soil area associated to CL1 (Soils on dune ridges and lagoon islands, formed by sands, from very to extremely calcareous) and CL2 (Soils on reclaimed lagoon areas, artificially drained, formed by very to extremely calcareous silts) classes in coastal municipalities of the Veneto Region for the reference period.

### 3.3.6 Permeability

Permeability of a receptor plays a significant role in defining its vulnerability to pluvial floods and coastal flooding. For the reference period, we retrieved the permeability data available from ARPAV in 2016, which is classified into 6 classes: no soil, low, moderately low, moderately high, high, and very high permeability. The explanation of the permeability classes is specified in Table 3. The risk assessment considers the total extension of the low and moderately low classes with permeability lower than 3.6 mm/h, given their sensitivity level to flood hazards. In fact, lower permeability soils are more vulnerable to floods because of its limited ability to infiltrate water, not only at higher risk to flood events and but also possessing a low recovery rate to floods (Sampson, 2015). The total area of these 2 classes of each municipality is summed up and divided to municipality's area to obtain their extent in each municipality.

Table 3. Description of the permeability classes.

Permeability class	Description
Very high	>360 mm/h
High	36-360 mm/h

Moderately high	3,6-36 mm/h
Moderately low	0,36-3,6 mm/h
Low	0,036-0,36 mm/h
No soil	Water

The map of the permeability indicator extracted for the Veneto coastal municipalities is shown in Figure 31 and the statistics for area with low and moderately low permeable soil (< 3.6 mm/h) is presented in Figure 32. There is a distribution of very high permeable soils along the coast of northern municipalities and a strip extended north-east to south-west, connecting Chioggia and the Po River (Figure 31). The distribution of this class is explained by the presence of the CL1 soil class - soils on dune ridges and lagoon islands, formed by sands, from very to extremely calcareous (Figure 29), which is characterized with very high permeable capacity.

The distribution of soils with a permeability lower than 3.6 mm/h is uneven within the municipalities (Figure 32). Northern municipalities, namely S.M. al Tagliamento, Caorle, and Eraclea have a significantly high proportion of low permeability, up to 70-80%. The most southern municipalities, including Porto Viro, Porto Tolle, and Ariano nel Polesine, also have a high proportion, ranging from 47% to 57%. On the other hand, the municipalities in the middle, namely Jesolo, Venezia, Chioggia, and Rosolina, have a lower proportion of low permeable soil (lower than 33%), whereas, in Cavallino-Treporti, there is no presence of low permeable soil.

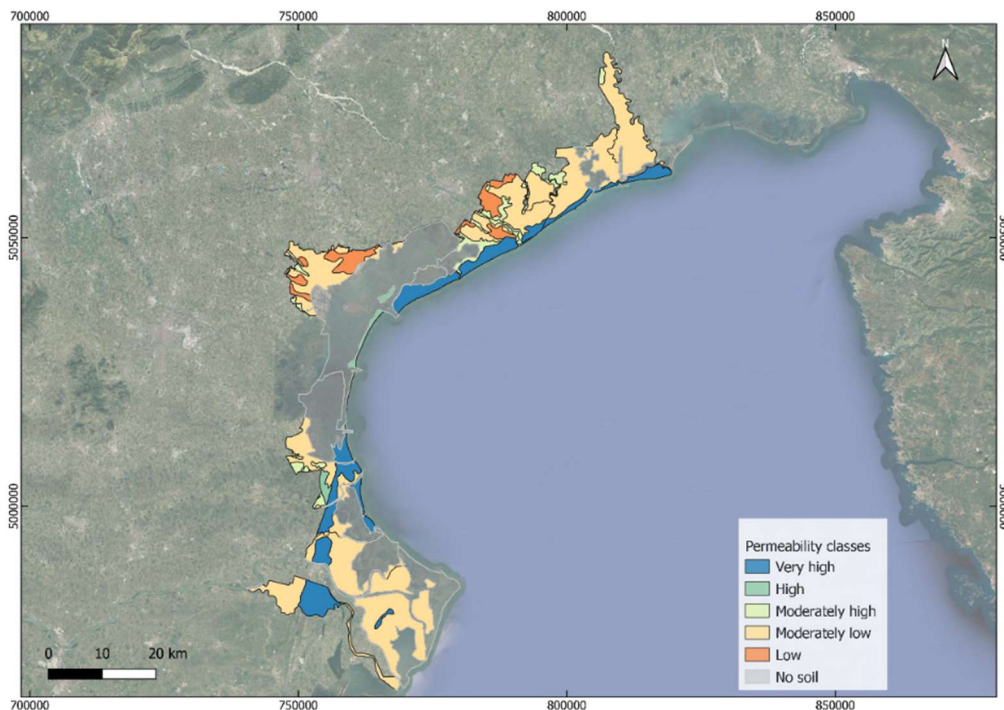


Figure 31. Map of the permeability indicator extracted for the Veneto coastal municipalities in the reference period.

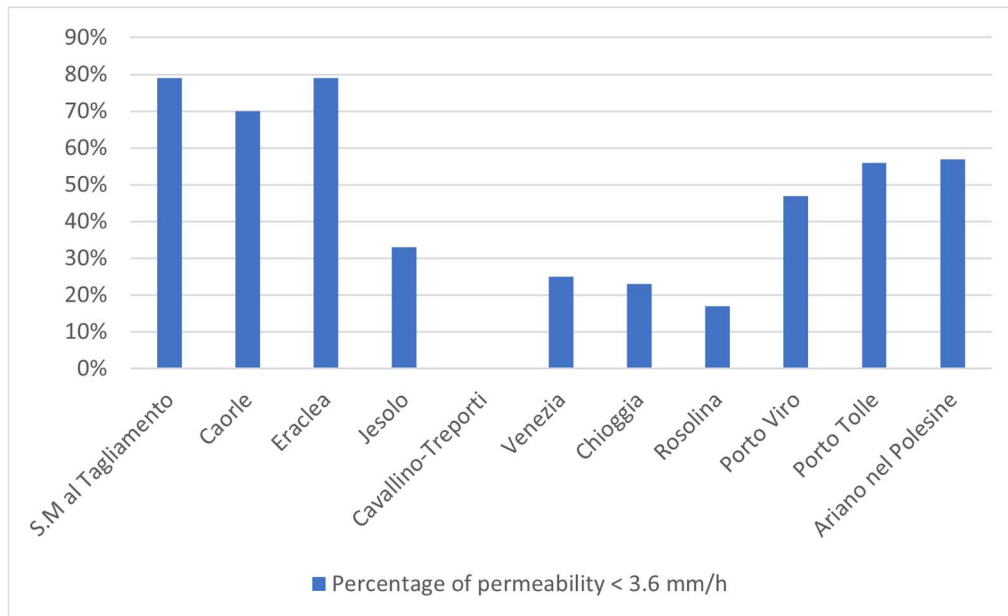


Figure 32. Percentage of area with low and moderately low soil permeability (< 3.6 mm/h) in Veneto coastal municipalities in the reference period.

### 3.3.7 River discharge

River discharge is defined as the volumetric flow rate of water that is transported through a given cross-sectional area (Buchanan & Somers, 1969). River discharge has a wide variability, and it is influenced by many factors, the most important of which are the atmospheric conditions (e.g., amount of precipitation, wind speed). Other factors that play an important role in the variability of the river discharge are the human activities, the type of soil, the surrounding vegetation, the steepness of the valley, the size of the drainage basin. Atmospheric conditions, human activities and drainage basin size influence both the average river discharge and its maximum; the other parameters influence the maximum leaving the average constant, because they influence the speed at which the water from precipitation collects in the river (Jackson, 2014).

High peaks of river discharge may be associated with inundation of the surrounding areas, although floodings are rare near the mouth of the rivers. Low levels of river discharge can lead to higher levels of seawater intrusion in the river mouth, with consequent alterations of the surrounding wetlands habitat. The total amount of river discharge overtime is an important factor for the evaluation of the marine water quality, as the amount of water influences the amount of sediments and the dissolved nutrients / contaminants, including human generated polluting agents (Interlandi & Crockett, 2003; Mcmillan et al., 2012).

The river discharge data in the Veneto pilot are provided by ARPAV and ARPAE:

- ARPAV provided river discharge data for rivers Livenza, Piave, Brenta and Adige for the timeframe 2009-2019;
- ARPAE provided river discharge data for the Po river for the timeframe 2009-2020;

The water flow is measured near the mouth of the river (except for the Po river, which is measured at Pontelagoscuro, about 75 km landward), and the provided value is the daily average of the water flow. Data for the Tagliamento and Sile rivers are not available.

The correspondence between the river and the municipality is depicted in Table 4.

*Table 4. Correspondence between rivers and municipalities.*

River	Municipality
Livenza	Caorle
Piave	Jesolo, Eraclea
Brenta	Chioggia
Adige	Chioggia, Rosolina
Po	Porto Tolle

As the assessment endpoints for this analysis are the damages caused by extreme weather events, the river discharge analysis is aimed to identify the dates in which each river is extremely full or extremely dry, rather than listing the actual flow rate. We would like to introduce this information in the analysis as we consider that damages could be generated by river flooding in case of very high river discharge, or by seawater intrusion in case of very low river discharge.

The map showing the main rivers in the Veneto Coastline is shown in Figure 33. Figure 34 shows the behavior of river discharge with time for the 6 municipalities; the comparison of the subplots highlights that the days with very high river discharge for the different rivers are the same for all the municipalities. From the observation of Figure 34, we can also note that peaks of river discharge are extremely high compared to the average of river discharge.

Figure 35 shows the distribution of river discharge for each municipality. We can observe from the plot that for all the municipalities the distribution is asymmetric (like a Poisson distribution), with the left tail (the one that starts at 0) much shorter than the right tail (the one associated with high values of the discharge). However, some municipalities (Caorle, and, to a lesser extent, Chioggia Rosolina, Porto Tolle) have a much higher variance (more variability) than the ones crossed by river Piave, which is often very dry (Jesolo, Eraclea).

From an environmental point of view, it is important to underline that, the north-south littoral current often brings fresh water to the south. On the other hand, the river discharge value is



measured near the river mouth (except for river Po), hence it is extremely influenced by the tidal range which affect the whole North Adriatic region.



Figure 33. Main rivers' network and mouth location within the Veneto territory along the Adriatic coast.

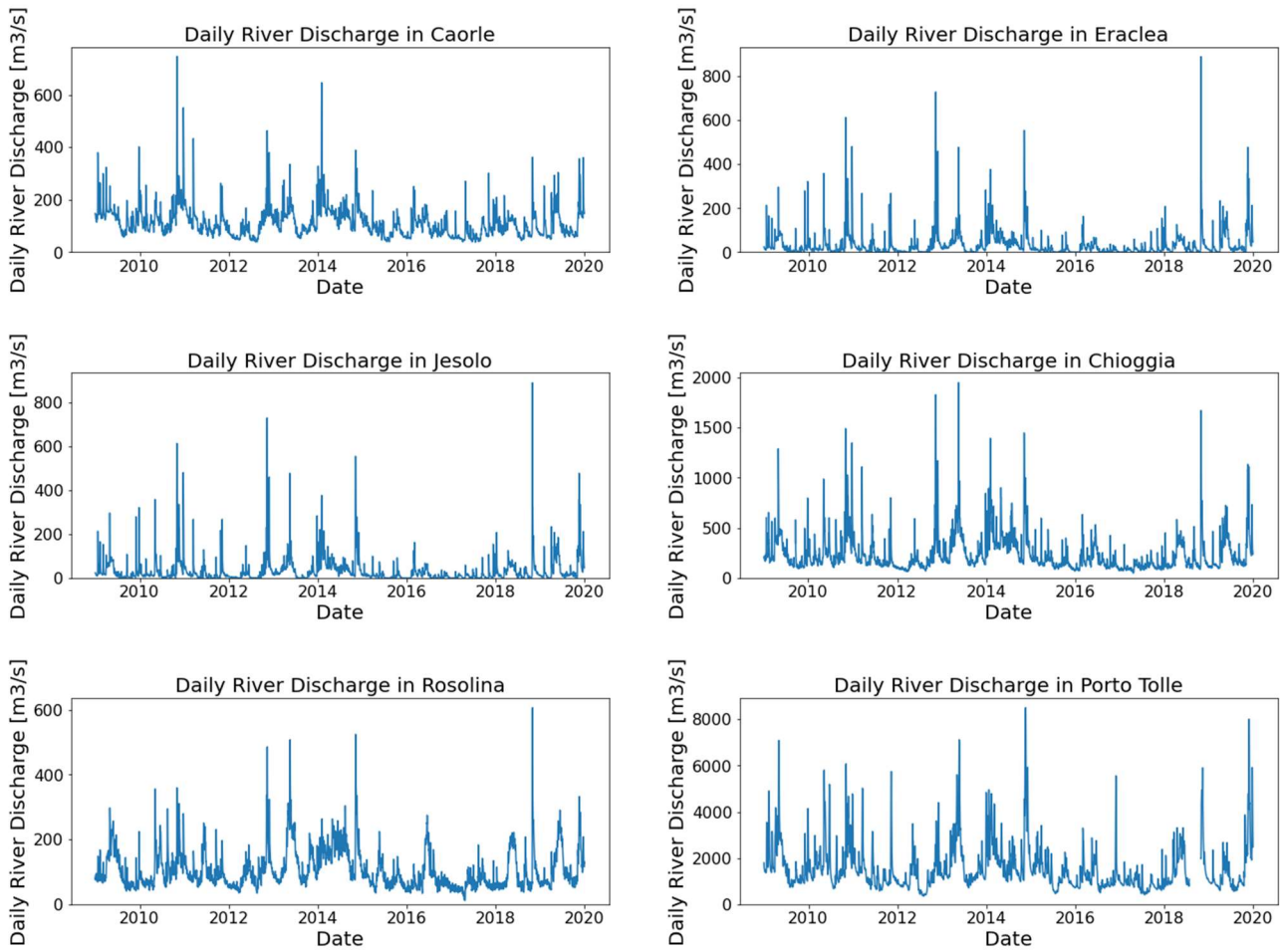


Figure 34. River discharge for the 6 municipalities.

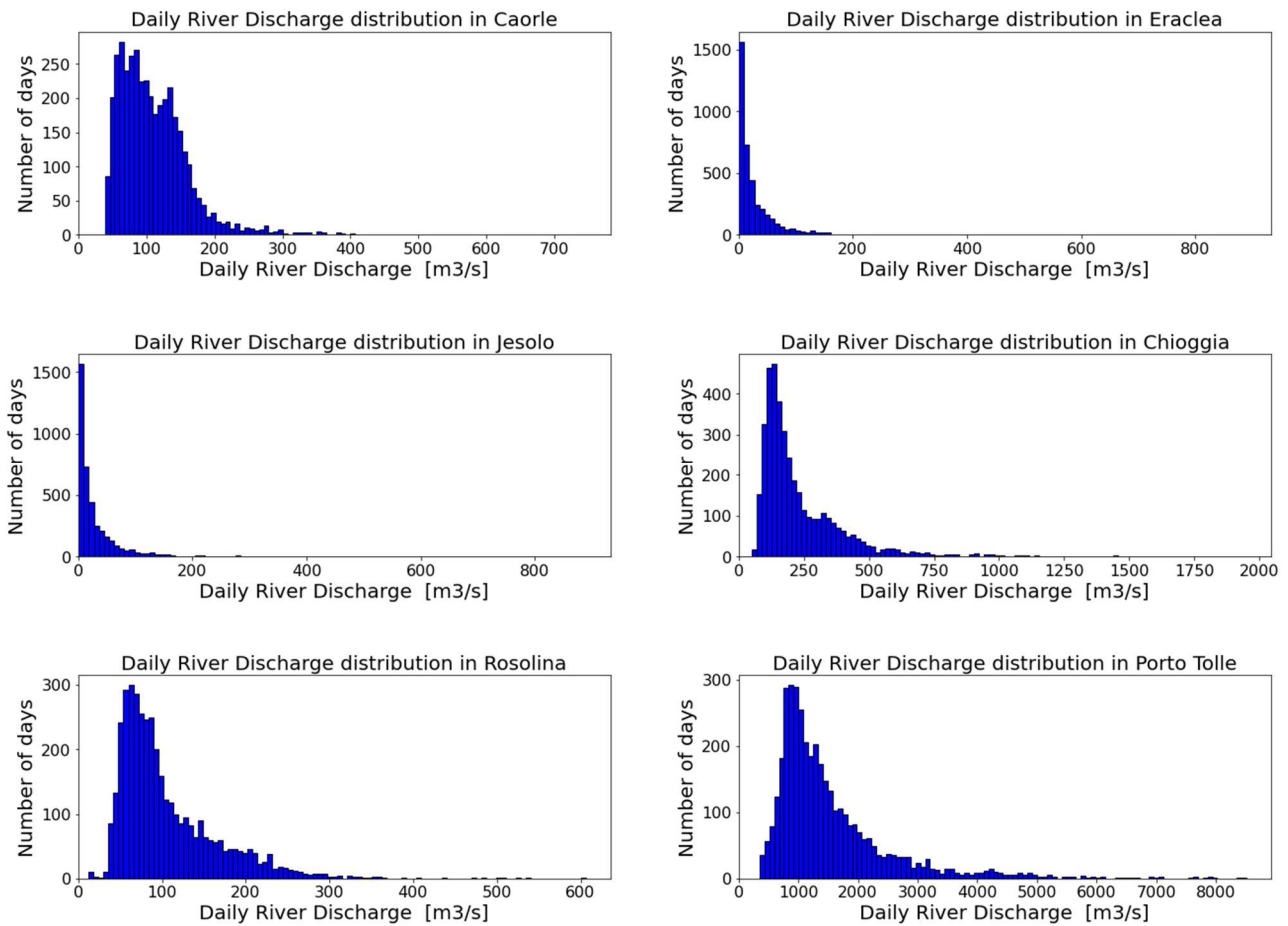


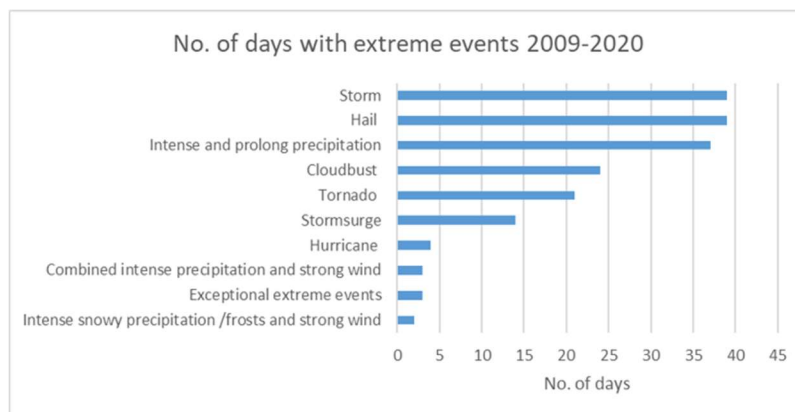
Figure 35. River discharge distribution for the 6 municipalities.

### 3.4 Damage indicators

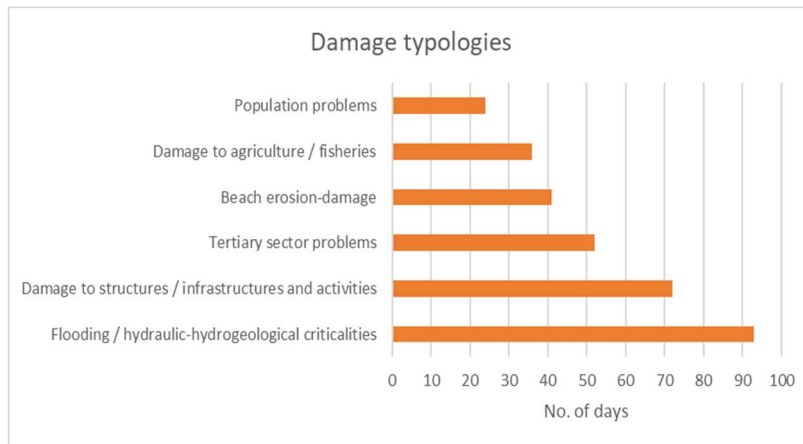
This section specifies indicators related to damages (e.g., flooding, beach erosion, agricultural losses) and services interruption (e.g., blackouts, impaired viability) caused by extreme climate change or meteorological events on the territory. The data were extracted by the DPGR (“Decreto del Presidente della Giunta Regionale”) documents which witness the activation of the “stato di crisi” at the regional level: the activation of this emergency state is consequent to significant damages caused by extreme weather events on the territory. These documents report qualitatively the damages/issues on involved elements at-risk at the municipality level after extreme events happening. Data are available for the period 2009-2020.

This indicator summarizes the damages and the services interruption caused by climate change or meteorological events on the municipality territory happened within the timeframe 2009-2020. In this period, the total number of events that caused damage (i.e., activation of ‘stato di crisi’) on the considered municipalities is 42, for a total of 103 days with a reported damage.

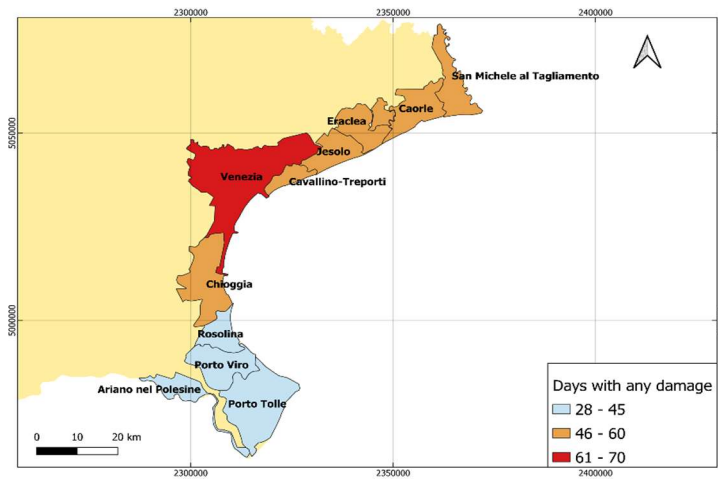
The most frequent extreme events leading to damages are represented in Figure 36a. Events related to extreme wind and precipitation were the most frequently recorded within the territory. Storms, hails, intense and prolong precipitation events were reported to be among the most recurrent ones causing damages. Six different typologies of damages (i.e., Flooding in urban areas, Damage to agriculture/fisheries, Population problems, Damage to beach, Damage to structures/infrastructures and activities and Tertiary sector problems) were recognized (Figure 36b). It can be noted that the most frequent (e.g., higher probability) is flooding in urban areas, that interested 93 days, followed by damage to structures/infrastructures and activities witnessed on 72 days. On the other hand, Figure 36c reports a classification of the total number of damages happened within each municipality. In general, the southern municipalities (Rosolina, Porto Viro, Porto Tolle and Ariano nel Polesine) present a significant lower total number of days with a damage within them territory in the considered timeframe. The municipality that registered the lower number of total days with a 64 damage is Ariano nel Polesine (30 days). Conversely, the northern municipalities present a higher number, with the Venice municipality reaching up to 73 total days with a damage.



(a)



(b)



(c)

Figure 36. Damage events reported in the Veneto coastal municipalities within 2009-2019 with the causal extreme events (a), damage typologies (b), and their frequency among the municipalities (c).

## 4 Primary vulnerability/exposure information layers used to inform climate impacts and adaptation analysis at the local scale

This section is aimed at describing territorial multi-vulnerability (MV) information layers to inform climate change impacts, as a condition defining the propensity of a territorial system to suffer damage induced by multiple climate stresses). MV aims to study the relationship between climate stresses and the territory, identifying some specific climate impacts. Considering three main weather-climate impacts (Urban Flooding, Coastal Flooding and Urban Heat Island) the methodology searches for the best geo-referenced data that can best describe the specific cumulative impact through testing a GIS-based multi-attribute exploratory procedure.

Specifically, spatial indicators are reported, focusing on the calculation of vulnerability and exposure variables, to test a climate-oriented spatial multi-hazard assessment.

As a consequence, they will be integrated into the multi-vulnerability (MV) and multi-risk assessment (MR) model developed to define climate-driven damages in the coastal areas of the Veneto Pilot (Cavallino Treporti, Jesolo and Porto Tolle Deliverable WP3\_5\_1 and WP5\_4\_5).

In this Section, we present a detailed description of the retrieved the following spatial indicators:

- Vegetation Health Index (VHI).
- Map of runoff coefficients (MCD).
- Digital Terrain Model (DTM).
- Imperviousness Density (IMD).
- European Settlement Map (ESM).
- Soil cover and soil cover database.

### 4.1 Spatial indicators

The workflow continues with data collection to select the morphological evaluation criteria used in the assessment methodology (MV and MR).

The evaluation methodology uses information and data from heterogeneous sources. They allow us to describe the profile of the urban-territorial system and to define the multi-vulnerability domain, referable to the three reference impacts: UHI, UF, and Ss. From an evaluation point of view, these three types of impact can be interpretative meta-criteria. Some data originate from remote sensing analysis algorithms, while others come from pre-packaged spatial information available in regional, provincial and European work/research settings (Table 5).

*Table 5. Information layers and base maps used for multi-vulnerability and multi-risk analysis*

Information level	Type	Resolution	Source	Year
Vegetation Health Index (VHI)*	Raster	30m x 30m	Landsat 8 (United States Geological Survey-USGS)	2020
Map of runoff coefficients (MCD)**	Raster	30 m x 30 m	Università Iuav di Venezia	2018
Digital Terrain Model (DTM)	Raster	25 cm x 25 cm	City Subway of Venice	2014
Imperviousness Density (IMD).	Raster	10m x 10m	Copernicus Programme	2018
European Settlement Map (ESM)	Raster	2m x 2m	Copernicus Programme	2015
Soil cover and soil cover database (CCS)	Shapefile		Wind Region	2018
Urban activities (OSM)	Shapefile		OpenStreetMao (OSM)	2021

\*Elaboration by the authors conducted on multispectral image "LC08\_L1TP\_191029\_20200730\_20200807\_01\_T1"

\*\*Elaboration on Veneto Region Land Cover database (CCS 2018). See Maragno, D. et al. (2020), 'Land-Sea Interaction: Integrating Climate Adaptation Planning and Maritime Spatial Planning in the North Adriatic Basin', *Sustainability*. MDPI, 12(13), p. 5319. doi: 10.3390/su12135319.

By combining the meta-criteria with the data in Table 5, it is possible to define a spatial multi-criteria approach, i.e. to recognize the spatial domain of MV. Specifically, the use of the data in Table 1 has a threefold purpose:

- Characterize the meta-criteria concerning the nature of the climate impact;
- Define the judgment criteria with which to evaluate the semantic domain;
- Evaluate and describe the relationship between urban morphologies and their susceptibility to climate impact.

The characterization of MV is defined by selecting a core set of morphological criteria suitable for recognizing vulnerability in a multi-impact key. In the following Table, a logical association between

MV “subject area”, interpretative meta-criteria and evaluative criteria are reported (see Maragno et al. 2023).

#### 4.1.1 Vegetation Health Index (VHI)

The Vegetation Health Index (VHI) is an indicator of the evolution and health status of vegetation, estimated based on the relationship between moisture values and thermal stress conditions. It provides a raster image that highlights areas with better vegetation and ecosystem health. This index assumes a standardized value ranging from 0 to 100 (expressed as a percentage). Low percentage values of VHI identify areas affected by potential stress due to specific conditions, such as drought induced by heat waves or rainfall conditions that disrupt vegetative well-being (Figure 37).

The VHI can also be considered as a sensitivity criterion, recognizing surface areas more prone to the consequences of heat waves. In this case, values corresponding to the complement to 100 are used.

The index is calculated using Landsat 8 satellite imagery. The estimation is indirect, as it is based on the vegetation response, both forest and agricultural, to thermal stress or variations in soil moisture. The VHI is obtained through the ratio of two derived satellite indices: the Temperature Condition Index (TCI) and the Vegetation Condition Index (VCI). The TCI calculation utilizes thermal data obtained from the Land Surface Temperature (LST), while the VCI calculation is based on vegetation data from the Normalized Difference Vegetation Index (NDVI), which reflects soil moisture conditions.



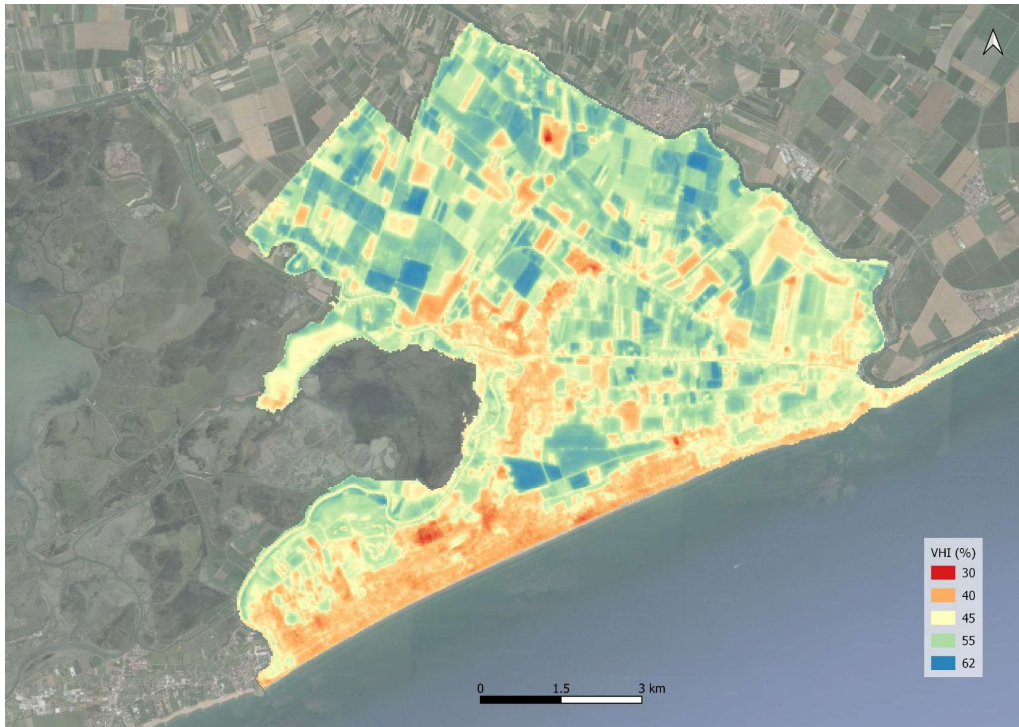


Figure 37. Vegetation Health Index of Jesolo (Source: Processing by Iuav, 2020).

#### 4.1.2 Map of runoff coefficients (MCD)

The estimation of hydraulic performance in a territory is often entrusted to specific simulation models of the 'inflow-outflow' dynamics. This methodology develops a logical model for the modelling of surface runoff based on a spatial association between land uses, terrain morphologies, and runoff coefficients.

The runoff coefficient is a hydraulic parameter that determines the transformation of inflows into outflows, given by the ratio between the volume discharged through an assigned section within a defined time interval and the meteoric volume precipitated within the same interval. The parameter is estimated in a defined watershed and is evaluated considering the permeability characteristics of the different surfaces present in the draining basin.

The runoff map is created through a schematization and reclassification of land uses (in this case, starting from the land use model of the Veneto Region: the CCS 2020) according to the permeability characteristics of the soils. The value is expressed as a percentage of rainfall that transforms into surface runoff (ranging from 0.1 to 0.9).

Land uses allow for the estimation of absorption coefficients and surface runoff coefficients of meteoric waters, identifying urban areas that are more predisposed and sensitive to the impacts generated by extreme weather events (Figure 38).

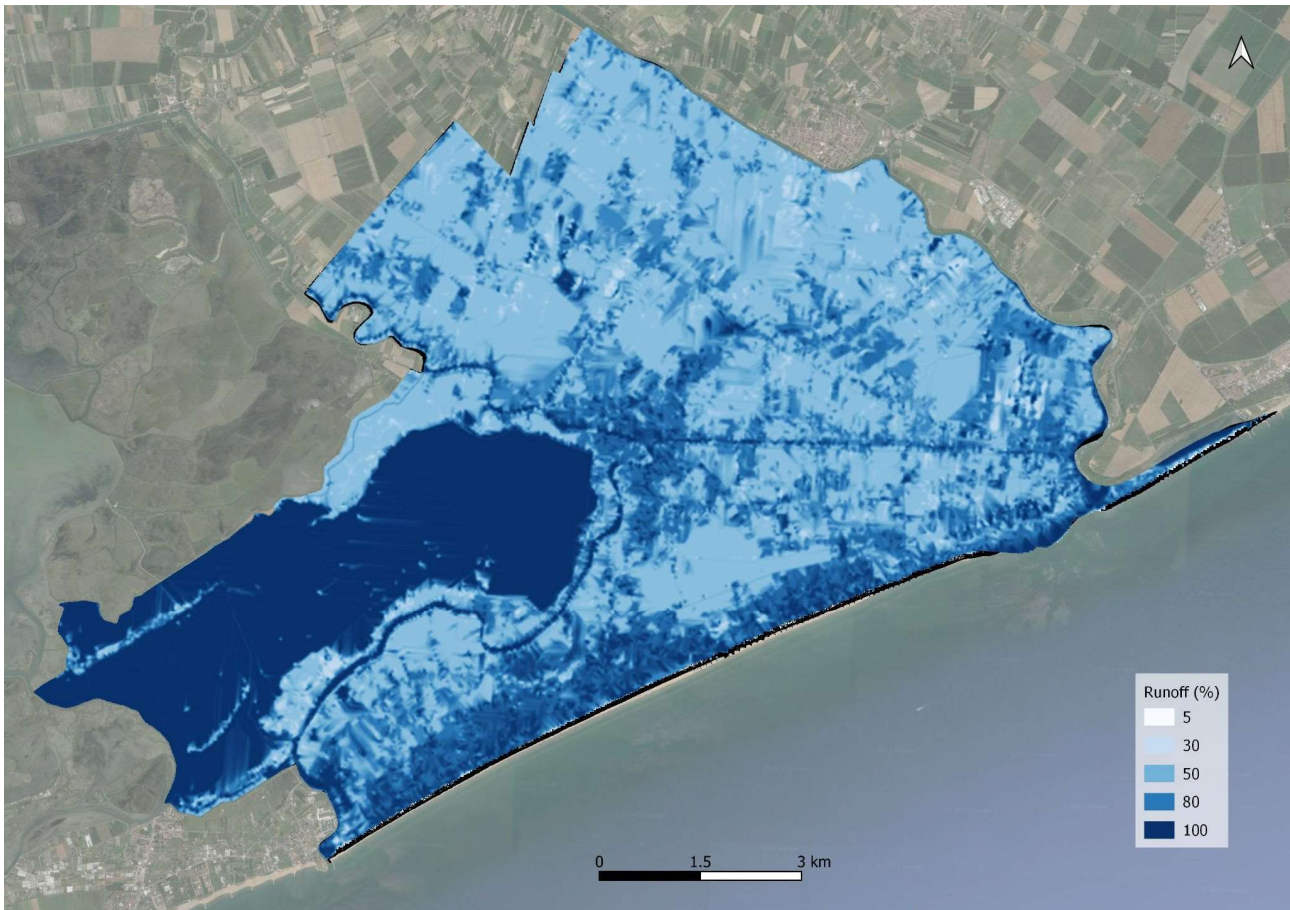


Figure 38. Map of surface runoff in Jesolo (Source: Processing by luav, 2020).

#### 4.1.3 Digital Terrain Model (DTM)

The Digital Terrain Model (DTM) with a resolution of 25 cm of the Metropolitan City of Venice (CMVE) is obtained through the processing of data derived from LiDAR scanning on an aerial platform (flight conducted in March 2014, Figure 39).

Within the analysis of multi-vulnerability, the use of the Digital Terrain Model (DTM) contributes to the identification of areas with high or low sensitivity to climate impacts. This data allows for the

identification of coastal areas with relatively low elevations, making them more susceptible to storm surges and sea-level rise.

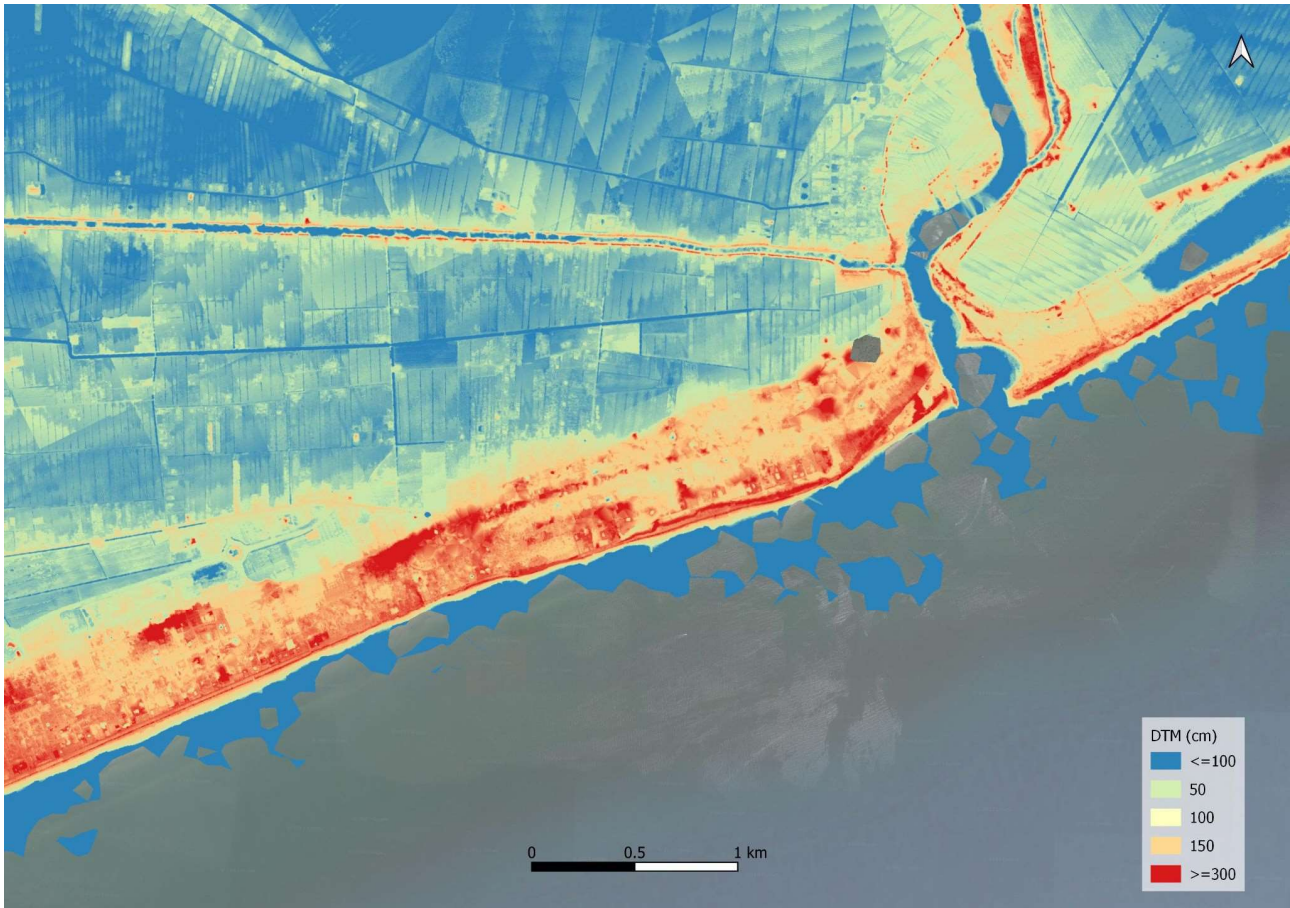


Figure 39. Digital Terrain Model 0.25 x 0.25: Coastal strip detail of Jesolo (Source: Città Metropolitana di Venezia, 2014).

#### 4.1.4 Imperviousness Density (IMD)

Indicator of impermeable land area as of 2018. The Impermeable Surface Density (IMD) is derived using a semi-automatic classification based on the calibration of the Normalized Difference Vegetation Index (NDVI). It estimates the percentage of impermeable land for each pixel. IMD is a raster dataset from the Copernicus Program that provides information on the level of soil impermeability. It has a spatial resolution of 10 meters. IMD ranges from 0 to 100 (Figure 40).

Within the multicriteria analysis, the IMD criterion helps define areas that are particularly vulnerable to heatwaves due to high levels of impermeability. Consequently, these areas are less

capable of absorbing surface runoff generated by intense rainfall events. Impermeable surfaces absorb solar radiation and contribute to the urban heat island effect. Urban flooding issues can be exacerbated by a high degree of impermeability. It is worth noting that the Copernicus program utilizes satellite imagery acquired from the Sentinel-2 platform to derive the IMD data.

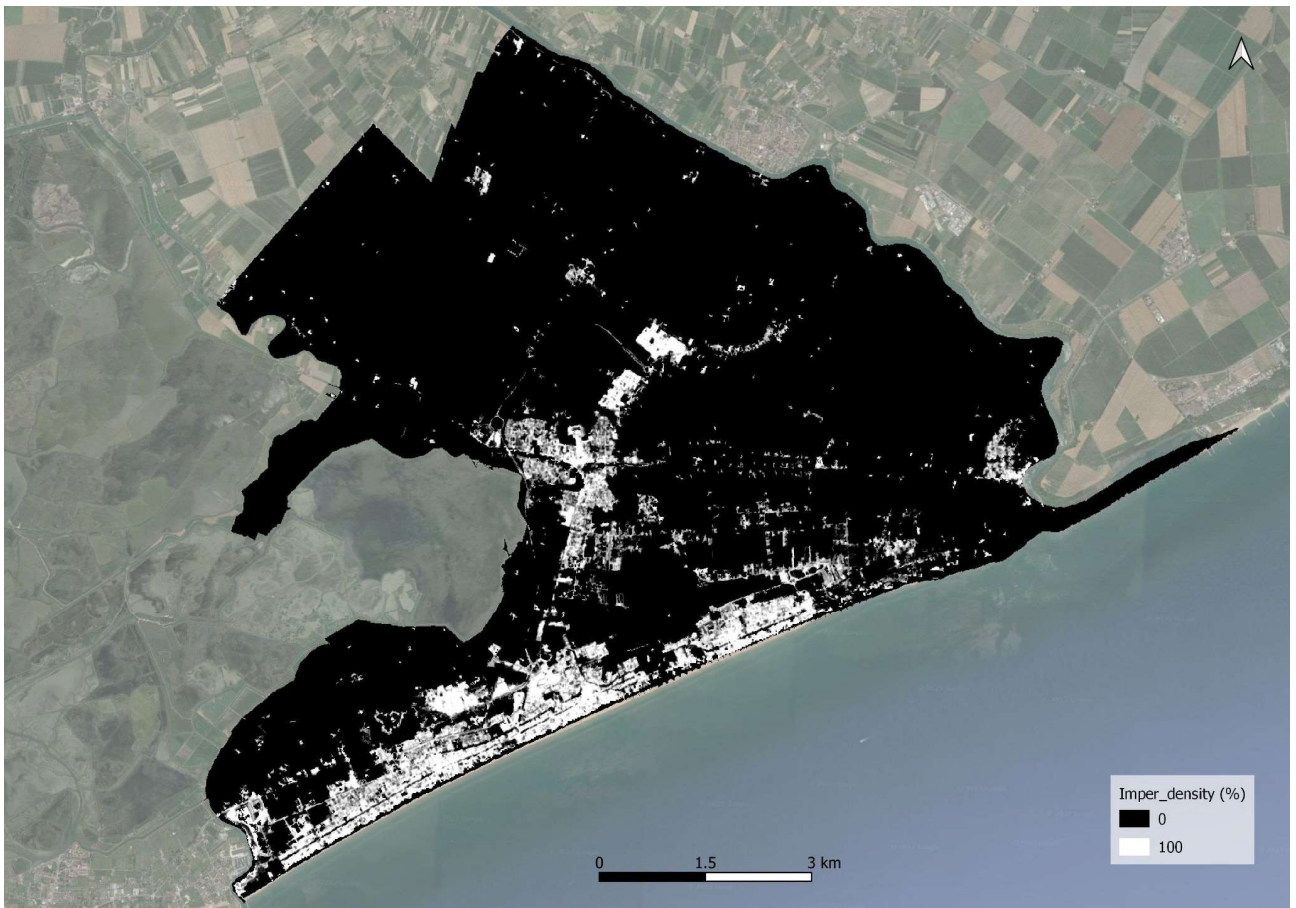


Figure 40. IMD Imperviousness HRL of Jesolo (Source: Copernicus Program, 2018).

#### 4.1.5 European Settlement Map (ESM)

The resulting map, the European Settlement Map (ESM), is a 2-meter raster map that expresses the proportion of the pixel area covered by buildings and was produced in 2015 (Figure 41). It was jointly developed by the Joint Research Centre (JRC) and the Directorate-General for Regional and Urban Policy (DG REGIO) of the European Commission to support policymakers.

It represents the highest-resolution continental map produced to date on a data-driven basis and involves the fully automatic extraction of image information based on textual and morphological analysis of the images. The learning method enables the processing of high-resolution image data using low-resolution thematic layers as a reference. Validation shows an overall accuracy of 96% with omission and commission errors below 4% and 1%, respectively.

This indicator is therefore linked to the compactness of buildings and implicitly connected to the presence of a high concentration of the population potentially vulnerable to the impacts of climate change. In settlement areas characterized by a high concentration and compactness of buildings, the spatial response to the climatic phenomenon may be significantly altered by urban morphologies and patterns, as well as factors characterizing building typologies.



Figure 41. European Settlement Map Jesolo: Coastal strip detail (Source: Copernicus Program, 2015).

#### 4.1.6 Soil cover and soil cover database (CCS)

The Soil Cover database is a regional statistical and cartographic source in vector format (Figure 42). The legend is structured into 5 macro-levels following the nomenclature of the European project Corine Land Cover (CLC). The database operates at a scale of 1:10000 with the territory classified into 174 classes (see Ccs 2020, Regione del Veneto).

This indicator enables the depiction of an important snapshot of places, aimed at describing urban morphology: forms, density, openness/closure, uses, and functions; urban structures and mobility strategies. This profiling helps in understanding the concepts of urban quality and social livability.

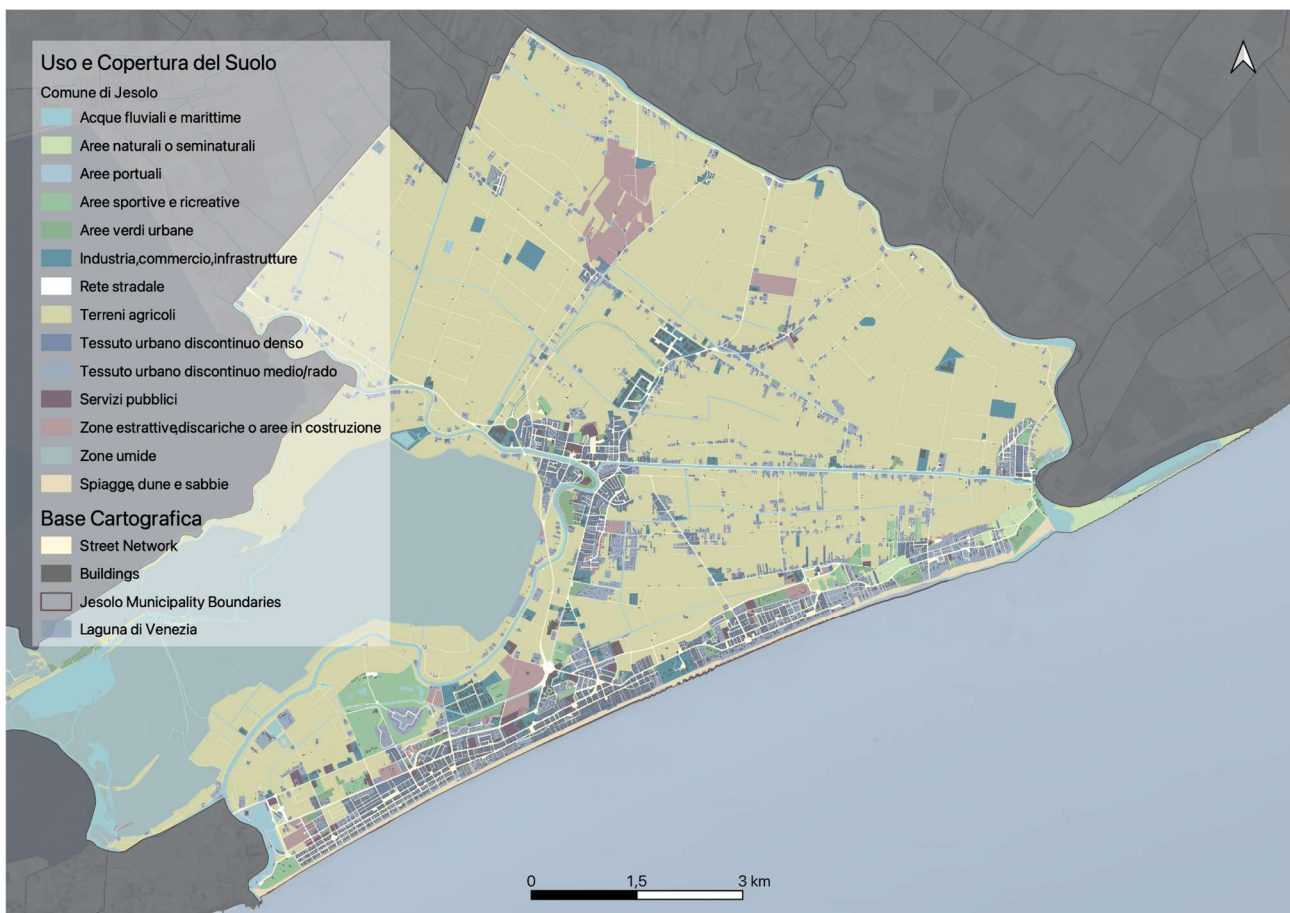


Figure 42. Land Cover and Land Use of Jesolo (Source: CCS 2020 - Veneto Region).

#### 4.1.7 Urban activities (OSM)

This is an indicator related to the construction of the map of exposure to climate change. The level of exposure is recognized through the structured detection of urban assets from the

OpenStreetMap (OSM) source. Exposure factors encompass infrastructure and economic assets, neighbourhood functions, and services that are necessary for the proper functioning of the urban fabric under study (Figure 43). The construction of the indicator utilizes Application Programming Interface (API) protocols and OSM tags (keywords). The OSM project tags include gastronomy; culture, entertainment, and art; historical objects; leisure, recreation, and sports; waste management; tourism and accommodation; finance; healthcare; communication; transportation; administrative facilities; shops and services. These twelve macro-categories allow for a certain homogeneity and coherence of spatial information directly linked to the functional profile of the urban space under investigation. Data collection occurs by specifying an export (or extraction) area.

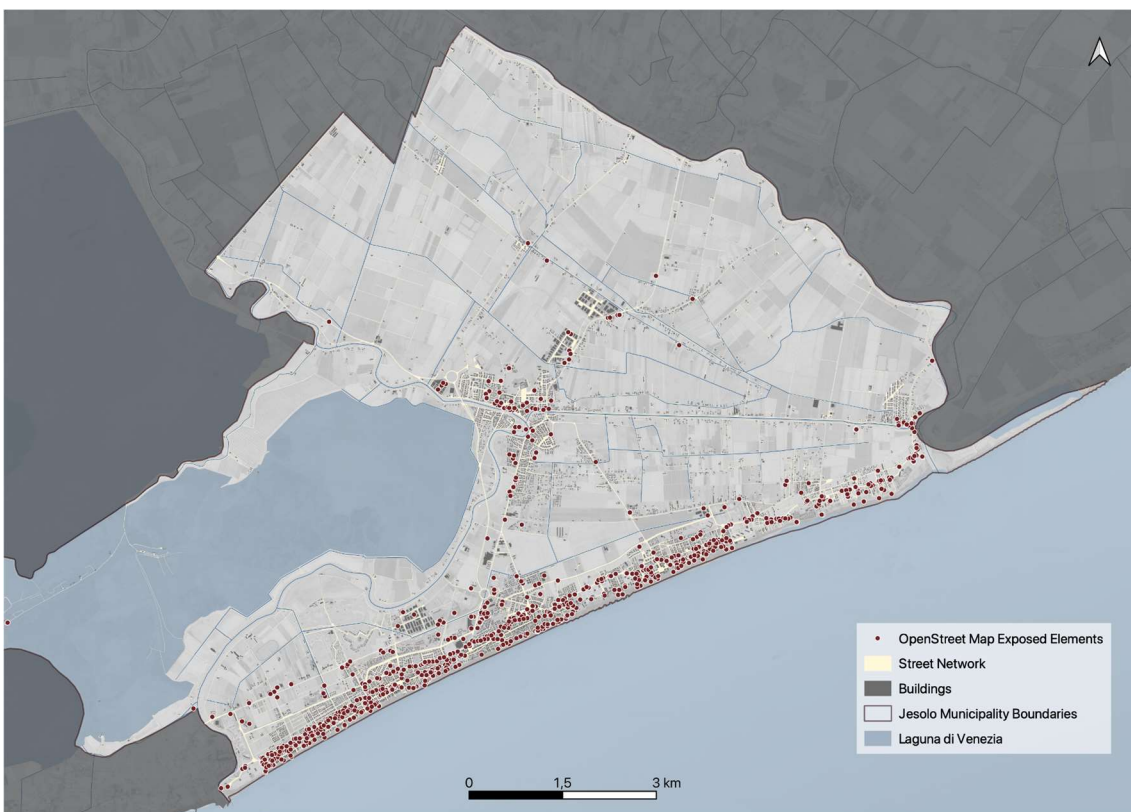


Figure 43. Land Cover and Land Use of Jesolo (Source: CCS 2020 - Veneto Region).